CAPITAL UNIVERSITY OF SCIENCE AND TECHNOLOGY, ISLAMABAD

MHD Mixed Convection in Aluminium - Water Nanofluid Filled Porous Cavity and Joule Heating

by

Sumbal Shahid

A thesis submitted in partial fulfillment for the degree of Master of Philosphy

in the

Faculty of Computing
Department of Mathematics

2019

This thesis is dedicated to my beloved mom, **Naila Shahid** who always keeps me motivated and positive whenever I got fed up with this and wanted to quit, to my father, **Shahid Hameed** for letting me reach at this level and finally to **Dr. Shafqat Hussain** for his patience throughout my work.

CERTIFICATE OF APPROVAL

MHD Mixed Convection in Aluminium-Water Nanofluid Filled Porous Cavity and Joule Heating

by

Sumbal Shahid

MMT163002

THESIS EXAMINING COMMITTEE

S. No.	Examiner	Name	Organization
(a)	External Examiner	Dr. Muhammad Sabeel Khan	IST, Islamabad
(b)	Internal Examiner	Dr. Abdul Rehman Kashif	CUST, Islamabad
(c)	Supervisor	Dr. Shafqat Hussain	CUST, Islamabad

Dr. Shafqat Hussain
Thesis Supervisor
May, 2019

Dr. Muhammad Sagheer
Head
Dept. of Mathematics
May, 2019

Dr. Muhammad Abdul Qadir
Dean
Faculty of Computing
May, 2019

Author's Declaration

I, **Sumbal Shahid** hereby state that my M.Phill thesis titled "**MHD Mixed Convection in Aluminium-Water Nanofluid Filled Porous Cavity and Joule Heating**" is my own work and has not been submitted previously by me for taking any degree from Capital University of Science and Technology, Islamabad or anywhere else in the country/abroad.

At any time if my statement is found to be incorrect even after my graduation, the University has the right to withdraw my MPhill Degree.

(Sumbal Shahid)

Registration No: MMT163002

Plagiarism Undertaking

I solemnly declare that research work presented in this thesis titled "*MHD Mixed Convection in Aluminium-Water Nanofluid Filled Porous Cavity and Joule Heating*" is solely my research work with no significant contribution from any other person. Small contribution/help wherever taken has been dully acknowledged and that complete thesis has been written by me.

I understand the zero tolerance policy of the HEC and Capital University of Science and Technology towards plagiarism. Therefore, I as an author of the above titled thesis declare that no portion of my thesis has been plagiarized and any material used as reference is properly referred/cited.

I undertake that if I am found guilty of any formal plagiarism in the above titled thesis even after award of M.Phill Degree, the University reserves the right to withdraw/revoke my M.Phill degree and that HEC and the University have the right to publish my name on the HEC/University website on which names of students are placed who submitted plagiarized work.

(Sumbal Shahid)

Registration No: MMT163002

Acknowledgements

All the praise and appreciation are for almighty **ALLAH** who is the most beneficent and the most merciful created the universe and blessed the mankind with Intelligence and wisdom to explore His secrets. Countless respect and endurance for **Prophet Muhammad (Peace Be Upon Him)**, the fortune of knowledge, who took the humanity out of ignorance and shows the right path.

I would like to show my gratitude and immeasurable respect to my supervisor **Dr. Shafqat Hussain**, Associate Professor, Capital University of Science and Technology, Islamabad who suggested the problem, extended all facilities and provided inspiring guidance for the success- ful completion of my research work. I deem it as my privilege to work under his able guidance.

I am extremely grateful to my teacher **Dr. Muhammad Sagheer**, **HOD** Mathematics department, Capital University of science and technology, Islamabad for his continuing beliefin my potential, for his encouraging and enthusiastic attitude and for many im- parted words of wisdom. I would also like to thank my respectable teachers **Dr. Rashid Ali**, **Dr. Abdul Rehman Kashif** and **Dr. Muhammad Afzal** for their encouragement and emphasis on striving for excellence when teaching mathematics.

My forever thanks goes to all research scholars, friends and colleagues in Mathematics lab for their friendship, help and providing a stimulating and encouraging environment. I wish to show my deep gratitude to my friends **Miss Maliha Atlas**, **Rakshanda Tariq**, **Hira**, **Mr.Bilal Ahmed** and **Maria Qamar** for moral support and personal interest.

At this juncture, I pay deep regards and thanks to my beloved parents, whose selfless care, love, devotion and prayers have made me able to achieve this goal. May Allah bless them.

(Sumbal Shahid)

Registration No: MMT163002

Abstract

In this work, the influence of Joule heating on MHD mixed convection in a square porous cavity having nanofluid together with thermal radiation has been analyzed. Vertical walls are supposed to be adiabatic and moving in the opposite directions with constant speed. Bottom wall is kept at hot temperature and the top wall is fixed at cold temperature. The Koo-Kleinstreuee-Lee (KKL) model is employed for the evaluation of effective thermal conductivity and dynamic viscosity of nanofluid. Impact of pertinent parameters in specific ranges such as Darcy number, Richardson number, radiation parameter, temperature ratio parameter, porosity parameter, Eckert number, Hartmann number and volume fraction of solid particles have been studied and presented in the form of isotherms, streamlines and plots. The dimensionless governing partial differential equations are discretized by using the Galerkin based finite element formulation.

Contents

List of Figures

List of Tables

Abbreviations

PDEs	Partial Differential Equations
BVP	Boundary Value Problem
FEM	Finite Element Method
FDM	Finite Difference Method
GFEM	Galerkin Finite Element Method

Symbols

symbol	**name(unit)**
C_p	Specific heat ($\mathrm{Jkg^{-1}K^{-1}}$)
d_s	Diameter of nanoparticle (nm)
Da	Darcy number,K/L^2
g	Gravitational acceleration ($\mathrm{m\ s^{-2}}$)
Gr	Grashof number,$\beta g \Delta T L^3/\nu_f^2$
L	Length of cavity (m)
k	Thermal conductivity ($\mathrm{W\ m^{-1}K^{-1}}$)
k_m	Effective thermal conductivity of porous medium ($\mathrm{W\ m^{-1}K^{-1}}$)
K	Permeability of porous media ($\mathrm{m^2}$)
Nu_{avg}	Average Nusselt number
Nu	Nusselt number (local)
p	Pressure ($\mathrm{N\ m^{-2}}$)
P	Dimensionless pressure
Pr	Prandtl number,ν_f/α_f
Re	Reynolds number, $V_w L/\nu_f$
Ri	Richardson number,Gr/Re^2
T	Demperature (K)
u, v	Dimensional velocity components ($\mathrm{m\ s^{-1}}$)
U, V	Dimensionless velocity components
V_w	Lid velocity
x, y	Dimensional space coordinates (m)
X, Y	Dimensionless space coordinates

Greek Symbols

α	Thermal diffusivity ($\mathrm{m^2s^{-1}}$)
β	Thermal expansion coefficient ($\mathrm{K^{-1}}$)
γ	Inclination angle of cavity(degree)
ϵ	Porosity of the porous medium
θ	Dimensionless temperature
μ	Dynamic viscosity ($\mathrm{kg\ m^{-1}s^{-1}}$)
μ_e	Equivalent viscosity of porous medium($\mathrm{kg\ m^{-1}s^{-1}}$)
ρ	Density($\mathrm{kg\ m^{-3}}$)
ν	Kinematic viscosity ($\mathrm{m^2s^{-1}}$)
ϕ	Volume fraction of the nanoparticles
avg	Average
c	Cold
f	Fluid
h	Hot
nf	Nanofluid
s	Nanoparticles

Chapter 1

Introduction

In this modern world, magnetic forces and mixed convective mode of heat transfer have received more importance and consideration in engineering sciences. Many scientist and engineers are trying to control convection phenomena in various situations for example in many metallurgical, nuclear and chemical processes and reactive polymer flows. They include other areas of interest in medical and engineering fields for example the crystal growth, microwave heating, magnetic resonance imaging (MRI) of mass transport process [1], electronic cooling, nuclear magnetic resonance (NMR) to petroleum exploration [2] and the nuclear waste management. The natural convection inside the porous enclosure filled with fluid numerically analyzed by Costa *et al.* [3] and concluded that the phenomena is effected by the magnetic field induced by two electric currents flowing parallel to the vertical surface of the cavity. Rahman *et al.* [4] have analyzed the MHD natural convection of heat transfer in a semi-circular cavity. The finite element method (FEM) was used to find the solution of the proposed problem. Ozoe and Okada [5] have analyzed the impact of free convection of heat transfer of molten gallium in cubic enclosure. Grosan *et al.* [6] have discussed the effect of internal heat generation and inclined magnetic field in free convection filled with copper-water nanofluid in a rectangular porous enclosure. It was concluded that for the parallel flow structure with the heat transfer source inside the cavity has strong conduction mode. Chamkha [7] has performed the simulation for the MHD flow in vertical walls considering heat generation and chemical reaction. Barron *et al.* [8] explored the impact of magnetic forces of free convection in a rectangular enclosure.

The situation where both the buoyant forces and pressure interact with each other is said to be mixed convection. Mixed convection is found in many engineering devices. Many fields of geophysical system such as the dynamics of lakes [9], heating and drying process [10], electronic equipment cooling [11], solar ponds [12] and float glass production [13] involve the mixed convection process. Khanafer and Chamka [14] examined the mixed convection flow in a porous enclosure filled with a fluid. It was concluded that the internal heat generation inside the cavity has significant effects on the isotherms and streamlines for small values of Richardson number. The impact of opposite thermal boundary conditions on mixed convection in a porous enclosure has been analyzed by Basak *et al.* [15]. The heating impact of mixed convection in the lid driven enclosure has been studied by Sivakumar *et al.* [16]. Shivasankaran *et al.* [17] also studied the lid driven enclosure with heating on both side of surfaces and found that there was direct relation on heat transfer rate.

A material containing the pores in it is said to be a porous medium.The term porosity is used in many fields including materials, engineering and earth sciences. The convection and conduction modes of heat transfer in a porous enclosure have been studied by Baytas *et al.* [18]. The working fluid in their problem was taken as air. The cavity consists of two vertical surfaces at opposite uniform temperatures and two horizontal conductive surfaces of finite thickness. Saeid [19] investigated the natural convection inside a porous enclosure whereas the vertical boundaries are isothermal at opposite temperatures. It was concluded that the Nu_{avg} was increased by increasing the values of Raleigh number. The natural convection in vertical cylinder bounded by solid walls has been studied by Sheremet and Trifonova [20].

Many researches [21, 22] investigated the nanofluids in different geometries with convective heat transfer. Koo-Kleinstreuer-Li (KKL) model and many other models have been proposed to compute the thermal conductivity and viscosity of the nanofluid. Salmam *et al.* [23], Ganji *et al.* [24] analyzed the heat transfer characteristics of nanofluid. The recent developments show that the nanofluid is an effective coolant for electronic devices. Koh and Colony [25] analyzed the microchannel as a porous medium by using Darcy equation. The impact of different aspect ratios on heat transfer rate in porous enclosure filled with copper-water nanofluid have been reviewed by Ghazvini and Shokouhmand [26].

Thermal radiation is the electromagnetic radiation which is emitted from a material due to the heat of the material. Most of the researchers analyzed the impact of the linear radiation [27]. Recently Dogonchi *et al.* [28] explored the impact of radiation on heat transfer of nanofluid flow in a porous medium. It was concluded that an increase in the velocity and decrease in the temperature profile were observed by increasing the Reynolds number and expansion ratio. Taseer *et al.* [29] have analyzed the impact of MHD nonlinear thermal radiation filled with nanofluid. Mixed convection and nonlinear thermal radiation filled with copper-water nanofluid have been discussed by Qayum *et al.* [30]. It was concluded that the heat transfer rate increases by increasing the values of mixed convection parameters. Sheikholeslami [31] also discussed the thermal radiations impacts on the nanofluid flow.

The passage of an electric current through a conductor produces heat is said to be Joule heating. Ohmic heating is another name of Joule heating. Currently, scientists and engineers are very concerned about increasing the efficiency of different industrial and mechanical systems. Hence, flow problem related with Joule heating in different physical aspects are discussed by many researchers. Mehmood *et al.* [32] discussed the magnetic forces and mixed convection in a square enclosure having blockage filled with nanofluid together with Joule heating. It was concluded that the gradual increment in the values of Eckert number and magnetic field strength increases the average temperature with in the enclosure. Mixed convection, magneto-hydrodynamic and Joule heating impacts in rectangular lid driven enclosure have been performed by Chowdhury *et al.* [33]. The impact of magneto-hydrodynamics in a square enclosure with a heated circular source together with Joule heating has been reported by Rehman *et al.* [34].

1.1 Thesis Contribution

The main purpose of the present study is to perform the numerical analysis for the mixed convection flow of nanofluid in a lid-driven enclosure. Impact of Joule heating are analyzed in the presence of magnetic field and different physical parameters such as Pr, Rd, Nr, Ri, Re, Ha and Ec on rate of heat transfer is examined. The problem consists of four coupled nonlinear partial differential equations that are solved by using Galerkin finite element technique. Graphical results are discussed and presented quantitatively to illuminate the solution.

1.2 Thesis Layout

This thesis is further divided into four chapters:

- **Chapter 2** includes few important definitions, laws and concepts that are helpful in understanding the work in third and fourth chapter.

- **Chapter 3** presents the review of the research paper of Mehmood *et al.* [35]. Mixed convection MHD flow in porous square enclosure filled with nanofluid. Galerkin finite element method has been applied for the nonlinear partial differential equations. Results are analyzed through streamlines, isotherms and

MATLAB graphs.

- **Chapter 4** extends the work of Mehmood *et al.* [35] by considering the effect of Joule heating in the energy equation. FEM is used to discretized the set of governing PDEs by using elements Q_2/P_1^{disc}. Various numerical results has been discussed for different physical parameters such as Ri, Re, Ec, Ha etc. The impact of governing parameters is analyzed through streamlines, isotherms and MATLAB graphs.

- **Chapter 5** summarizes the work and concludes the dissertation.

All the references used in this thesis are listed at the end.

Chapter 2

Some Important Definitions

This chapter contains the basic definitions, concepts, governing laws relating to the fluid mechanics ([36], [37], [38], [39], [40], [41]) and heat transfer phenomena [42]. Moreover, the fundamental of finite element method [43] used for the numerical estimation of the given problem is also discussed.

2.1 Fluid Flows and Related Terminologies

Definition 2.1. (**Fluid**)
"A fluid is a substance that deforms continuously under the application of a shear (tangential) stress no matter how small the shear stress may be. Because the fluid motion continues under the application of a shear stress, we can also define a fluid as any substance that cannot sustain a shear stress when at rest."

Definition 2.2. (**Fluid Mechanics**)
"The fluid mechanics is defined as the science that deals with the behavior of fluids at rest (fluid statics) or in motion (fluid dynamics), and the interaction of fluids with solids or other fluids at the boundaries."

Definition 2.3. (**Fluid Statics**)
"The branch of mechanics that deals with bodies at rest is called statics."

Definition 2.4. (**Fluid Dynamics**)

"The branch that deals with bodies in motion is called dynamics."

Definition 2.5. (**Density**)

"Density is defined as mass per unit volume.The density of a substance, in general, depends on temperature and pres- sure. The density of most gases is proportional to pressure and inversely proportional to temperature. Liquids and solids, on the other hand, are essentially incompressible substances, and the variation of their density with pressure is usually negligible." Mathematically it can be written as

$$\rho = \frac{m}{\bar{V}}. \tag{2.1}$$

Definition 2.6. (**Pressure**)

"The pressure in a fluid at rest at a given point is the same in all directions, and we define pressure as the normal component of force per unit area." It is expressed by P and mathematically, it can be written as

$$P = \frac{F}{A}, \tag{2.2}$$

where A is area and F is applied force.

Definition 2.7. (**Viscosity**)

"Viscosity is defined as the property of a fluid which offers resistance to the movement of one layer of fluid over another adjacent layer of the fluid." It is represented by μ and mathematically, it can be written as

$$\mu = \frac{\text{shear stress}}{\text{shear strain}}. \tag{2.3}$$

Definition 2.8. (**Kinematic Viscosity**)

"It is defined as the ratio between the dynamic viscosity and the density of fluid. It is denoted by the greek symbol (ν) called nu." It can be written as

$$\nu = \frac{\mu}{\rho}. \tag{2.4}$$

2.2 Classification of Fluids

Definition 2.9. (**Ideal Fluid or Inviscid Fluid**)

"A fluid, which is incompressible and is having no viscosity is known as an ideal fluid."

Definition 2.10. (**Real Fluid or Viscous Fluid**)

"A fluid, which possesses viscosity, is known as real fluid ."

Definition 2.11. (**Newtonian Fluid**)

"Fluids for which the rate of deformation is proportional to the shear stress are called Newtonian fluids. Most common fluids such as water, air, and gasoline are Newtonian under normal conditions."

Definition 2.12. (**Non – Newtonian Fluid**)

"Fluids for which the shearing stress is not linearly related to the rate of shearing strain are designated as non-Newtonian fluids." The examples of non-Newtonian fluid are blood, toothpaste, custard, ketchup, shampoo and honey. Mathematically it can be written as

$$\tau_{yx} \propto \left(\frac{du}{dy}\right)^n, n \neq 1$$
$$\tau_{yx} = \mu \left(\frac{du}{dy}\right)^n,$$

where, μ is apparent viscosity and n is the index of flow behaviour.

2.3 Types of Flows

Definition 2.13. (**Flow**)

"Flow is defined as the quantity of fluid (gas, liquid or vapour) that passes a point per unit time." Many types of flow are given below:

Definition 2.14. (**Laminar Flow**)

"The highly ordered fluid motion characterized by smooth layers of fluid is called laminar. The word laminar comes from the movement of adjacent fluid particles together in "laminates." The flow of high-viscosity fluids such as oils at low velocities is typically laminar."

Definition 2.15. (**Turbulent Flow**)
"The highly disordered fluid motion that typically occurs at high velocities and is characterized by velocity fluctuations is called turbulent. The flow of low-viscosity fluids such as air at high velocities is typically turbulent."

Definition 2.16. (**Steady Flow**)
"The term steady implies no change at a point with time." Mathematically, it can be expressed as

$$\frac{d\eta^*}{dt} = 0, \tag{2.5}$$

where η^* is fluid property.

Definition 2.17. (**Unsteady Flow**)
"The opposite of steady is unsteady. The term unsteady implies change at a point with time." Mathematically, it can be expressed as

$$\frac{d\eta^*}{dt} \neq 0, \tag{2.6}$$

where η^* is fluid property.

Definition 2.18. (**Compressible Flow**)
"When density variations within a flow are not negligible, the flow is called compressible. The most common example of compressible flow concerns the flow of gases."

Definition 2.19. (**Incompressible Flow**)
"Incompressibility is an approximation, and a flow is said to be incompressible if the density remains nearly constant throughout. Therefore, the volume of every portion of fluid remains unchanged over the course of its motion when the flow (or the fluid) is incompressible."

Definition 2.20. (**Uniform Flow**)

"Uniform flow is defined as that type of flow in which the velocity at any given time does not change with respect to space (i.e length of direction of the flow)."

Definition 2.21. (**Non – Uniform Flow**)

"Non-uniform flow is that type of flow in which the velocity at any given time changes with respect to space."

Definition 2.22. (**Internal Flow**)

"The flow in a pipe or duct is internal flow if the fluid is completely bounded by solid surfaces."

Definition 2.23. (**External Flow**)

"The flow of an unbounded fluid over a surface such as a plate, a wire, or a pipe is external flow."

2.4 Heat Transfer Phenomenon and Related Properties

Definition 2.24. (**Conduction**)

"Conduction is the transfer of heat from one part of a body at a higher temperature to another part of the same body at a lower temperature, or from one body at a higher temperature to another body in physical contact with it at a lower temperature. The conduction process takes place at the molecular level and involves the transfer of energy from the more energetic molecules to those with a lower energy level. This can be easily visualized within gases, where we note that the average kinetic energy of molecules in the higher-temperature regions is greater than that of those in the lower-temperature regions." Metals are good conductors.

Definition 2.25. (**Convection**)

"Convection, sometimes identified as a separate mode of heat transfer, relates to the transfer of heat from a bounding surface to a fluid in motion, or to the heat transfer across a flow plane within the interior of the flowing fluid."

It is further divided into three categories that are given below:

Definition 2.26. (**Force Convection**)

"If the fluid motion is induced by a pump, a blower, a fan, or some similar device, the process is called forced convection." Forced convection is the method of energy transportation in which fluid is forced to move using an external source.

Definition 2.27. (**Natural Convection**)

"If the fluid motion occurs as a result of the density difference produced by the temperature difference, the process is called free or natural convection. Natural convection is the motion that results from the interaction of gravity with density differences within a fluid."

Definition 2.28. (**Mixed Convection**)

"Mixed convection occurs when both natural convection and forced convection play significant roles in the transfer of heat. In applications it is important to first establish whether satisfactory predictions will result by ignoring either one, or if the combined effects must be considered."

Definition 2.29. (**Radiation**)

"Radiation, or more correctly thermal radiation, is electromagnetic radiation emitted by a body by virtue of its temperature and at the expense of its internal energy. Thus thermal radiation is of the same nature as visible light, x rays, and radio waves, the difference between them being in their wavelengths and the source of generation." Examples of radiation is the heat from the sun, or heat released by filament of the bulb.

Definition 2.30. (**Thermal Conductivity**)

"The property of a material to conduct heat is the Thermal conductivity.It is denoted by k. Thermal resistivity is the reciprocal of thermal conductivity .Heat transfer occurs at a lower rate in materials of low thermal conductivity than in materials of high thermal conductivity." Copper ia an example of metals with high thermal conductivity.

$$\frac{dQ}{dt} = -kA\frac{dT}{dx}. \tag{2.7}$$

Definition 2.31. (**Thermal Diffusivity**)

"It measures the ability of material to conduct thermal energy relative to its ability to store thermal energy means how fast or how easily heat can penetrate an object or substance." Mathematically, it is given as

$$\alpha = \frac{k}{\rho C_p}. \tag{2.8}$$

2.5 Dimensionless Numbers

Definition 2.32. (**Reynolds Number** (Re))

"This number expresses the ratio of the fluid inertia force to that of molecular friction (viscosity). It characterizes the hydrodynamic conditions for viscous fluid flow. With large Re numbers, the dynamic flow effect cannot be equalized by viscous friction and the flow stability is lost, which is manifested by swirls and turbulence in the fluid." The Re is expressed as

$$Re = \frac{\rho V_w L}{\mu} = \frac{V_w L}{\nu}. \tag{2.9}$$

where, V_w is lid velocity, ν is kinematic viscosity and L is length of cavity.

Definition 2.33. (**Prandtl Number** (Pr))

"This number expresses the ratio of the momentum diffusivity (viscosity) to the thermal diffusivity. It characterizes the physical properties of a fluid with convective and diffusive heat transfers." It is named after Ludwig Prandtl. The Prandtl number is written as

$$Pr = \frac{\nu}{\alpha} \tag{2.10}$$

Definition 2.34. (**Richardson Number** (Ri))

"It expresses the ratio of buoyancy effects to vertical slip effects." It can be written as

$$Ri = \frac{Gr}{Re^2}. \tag{2.11}$$

Definition 2.35. (**Raleigh number** (Ra))

"It characterizes the free convection heat transfer along a heat-exchanging surface.

It expresses the buoyancy-to-diffusion ratio or, alternatively, the free convection thermal instability in fluids.” It is a dimensionless number introduced by Lord Raleigh. It is denoted by Ra and mathematically it can be written as

$$Ra = \frac{g\beta(T_h - T_c)L^3 Pr}{\nu^2}, \tag{2.12}$$

where g, β, L^3 and ν represents the gravitational acceleration, volume expansion coefficient, characteristic length and kinematic viscosity.

Definition 2.36. (**Darcy number** (Da))
“The effect of permeable medium on the cross-sectional area (commonly squared diameter) on a fluid is known as Darcy number. It is named after Henry Darcy.” It is expressed as

$$Da = \frac{K}{L^2}. \tag{2.13}$$

where, K is permeability of porous media and L is length of cavity.

Definition 2.37. (**Hartmann number** (Ha))
“It is an important criterion of magneto-hydrodynamics. It expresses the ratio of the induced electrodynamic (magnetic) force to the hydrodynamic force of the viscosity or, alternatively, the ratio of the ponderomotive force (the electromagnetic volume force by means of which the magnetic field acts on a conductor through which electric current flows, which causes magnetic pressure) to the molecular friction force.” Mathematically, it is given as

$$Ha = BL\sqrt{\frac{\sigma_f}{\mu_f}}. \tag{2.14}$$

Definition 2.38. (**Grashof number** (Gr))
“It expresses the ratio of the product of inertia and buoyancy forces to the square of a viscous force.” This correlation is known as Grashof number (Gr). Mathematically,it is expressed as

$$Gr = \frac{g\beta(T_s - T_\infty)L^3}{\nu^2}. \tag{2.15}$$

Definition 2.39. (**Eckert number** (Ec))

"It expresses the ratio of kinetic energy to a thermal energy change." It can be written as

$$Ec = \frac{V_w^2}{(C_p)_f(T_h - T_c)}. \tag{2.16}$$

Definition 2.40. (**Porous medium**)

"It characterizes the porous environment behaviour with convective and mixed convective radiation flow and interaction in vertical porous canals. It occurs, for example, in magneto-hydrodynamics and is accompanied by entropic changes." A material containing the pores in it is called a porous medium. A porous medium is often considered by its porosity. Pores are usually filled with fluid, that is liquid and gases.

Definition 2.41. (**Nusselt Number** (Nu))

"It expresses the ratio of the total heat transfer in a system to the heat transfer by conduction. In characterizes the heat transfer by convection between a fluid and the environment close to it or, alternatively, the connection between the heat transfer intensity and the temperature field in a flow boundary layer. It expresses the dimensionless thermal transference." It is introduced by Wilhelm Nusselt. Mathematically, it is given as

$$Nu = \frac{hL}{k}. \tag{2.17}$$

where, L is the characteristic length, h denotes convective heat transfer and k is thermal conductivity.

2.6 Basic Governing Equations

2.6.1 Continuity Equation

"The continuity equation in this form describes the rate of change of density at a fixed point in the fluid. The continuity equation is developed from the law of conservation of mass. Mathematically, it is described as

$$\frac{\partial \rho}{\partial t} + \nabla.(\rho V) = 0. \tag{2.18}$$

For incompresible fluid, the continuity equation is written as

$$\nabla.V = 0.\text{''} \tag{2.19}$$

2.6.2 Law of Conservation of Momentum

"Each particle of fluid which is in state of steady or accelerated motion obey Newton second law of motion. This law states that the combination of all applied external forces acting on an object is equal to time rate of change of its linear momentum. This law can be given as

$$\rho \frac{dV}{dt} = \text{div } \tau + \rho b. \tag{2.20}$$

For Navier-Stokes Equation

$$\tau = -pI + \mu A_1, \tag{2.21}$$

where A_1 is the tensor and first time it was defined by Rivlin-Erickson

$$A_1 = \text{grad } V + (\text{grad } V)^t. \tag{2.22}$$

In the above equations, $\frac{d}{dt}$ denotes material time derivative or total derivative, ρ denotes density, V denotes velocity, p the pressure, b is body forces, μ is the dynamic viscosity and τ here denotes the Cauchy stress tensor. Cauchy stress tensor is expressed in the matrix form as

$$\tau = \begin{pmatrix} \sigma_{xx} & \tau_{yx} & \tau_{zx} \\ \tau_{xy} & \sigma_{yy} & \tau_{zy} \\ \tau_{xz} & \tau_{yz} & \sigma_{zz} \end{pmatrix}, \tag{2.23}$$

where $\sigma_{ii}, i = (x, y, z)$are normal stresses, otherwise the shear stress. For two dimensional flow, we have $V = [u(x, y, 0), v(x, y, 0), 0]$ and thus

$$\text{grad } V = \begin{pmatrix} \frac{\partial u}{\partial x} & \frac{\partial u}{\partial y} & 0 \\ \frac{\partial v}{\partial x} & \frac{\partial v}{\partial y} & 0 \\ 0 & 0 & 0 \end{pmatrix} \tag{2.24}$$

$$\frac{\partial u}{\partial t} + u\frac{\partial u}{\partial x} + v\frac{\partial u}{\partial y} = -\frac{1}{\rho}\frac{\partial p}{\partial x} + \nu\left(\frac{\partial^2 u}{\partial x^2} + \frac{\partial^2 u}{\partial y^2}\right), \tag{2.25}$$

Similarly, by repeating the above process for y component as follows:

$$\frac{\partial v}{\partial t} + u\frac{\partial v}{\partial x} + v\frac{\partial v}{\partial y} = -\frac{1}{\rho}\frac{\partial p}{\partial y} + \nu\left(\frac{\partial^2 v}{\partial x^2} + \frac{\partial^2 v}{\partial y^2}\right).\text{''} \tag{2.26}$$

2.6.3 Energy Equation

"For a stationary volume element through which a pure fluid is flowing, the energy equation reads.

$$\rho C_p\left(\frac{\partial}{\partial t} + V\nabla\right)T = k\nabla^2 T + \tau L_1 + \rho C_p\left[D_B\nabla C.\nabla T + \frac{D_T}{T_m}\nabla T\right], \tag{2.27}$$

where ρ_f represents the density, $(C_p)_f$ denotes the specific heat of basic fluid, $(C_p)_s$ represents the material of specific heat, L_1 is the rate of strain tensor, T is temperature, D_B is the Brownian motion coefficient, D_T represent the temperature diffiusion coefficient and T_m denote the mean temperature. The expression for Cauchy stress tensor τ for the incompressible fluid is expressed by

$$\tau = -pI + \mu A_1, \tag{2.28}$$

where A_1 is the tensor, μ is dynamic viscosity, p is pressure.

$$A_1 = \text{grad } V + (\text{grad } V)^t, \tag{2.29}$$

where t represents transpose of the matrix for two dimensional field velocity, τ is the Cauchy stress tensor.

$$\tau = \begin{pmatrix} \sigma_{xx} & \tau_{yx} & \tau_{zx} \\ \tau_{xy} & \sigma_{yy} & \tau_{zy} \\ \tau_{xz} & \tau_{yz} & \sigma_{zz} \end{pmatrix}.\text{''} \tag{2.30}$$

2.7 Finite Element Method

The finite element method (FEM) was first introduced by Clough [43]. It subdivides a large problem into collection of smaller parts, known as the finite elements. The FEM transforms the governing equations in to an appropriate form known as weak formulation or variational form.
The Galerkin weighted residual method is utilized for the implementation of FEM. In this method, the weight functions are chosen to be the trial functions themselves. The steps for the implementation of FEM based on the Galerkin residual technique are summarized as follows:

1. Both sides of governing equation is multiplied by the test function, that is vanishing on the boundary of the domain.

2. Use integration by parts to transform the higher order of differentiation from the unknown variable U to the test function w.

3. Include natural boundary conditions in the boundary integrals and the essential boundary conditions to the trial space. This is known as weak formulation.

4. Generate mesh or triangulation which divides the entire domain into non-overlapping elements. In one dimension, the mesh is a set of points that is, $x_0 = 0, x_1, x_2, \ldots x_N = 1$, where x_i is said to be a node and $e_i = (x_i, x_{i+1})$ is an element such that $e_i \cap e_j = \varphi$ for $i \neq j$. $h_i = x_i - x_{i-1}$ for $i = 0,\ 1, \ldots N$ is known as mesh size.

5. Approximate the infinite dimensional trial space U and test space W by finite dimensional spaces U_h and W_h, respectively where
   U_h(finite dimensional space)$\subset U$ (solution space).

6. Now we choose the basis functions $\varphi_1, \varphi_2, ...\phi_N$ of w_h, so that every test functions $w_h \epsilon W_h$ can be described as $w_h = \sum_{i=1}^{N} w_i\varphi_i \epsilon W_h$.

7. Find $u_h \epsilon U_h$ in such away $(u_h, w_h) = b(w_h) \; \forall \; w_h = \sum_{i=1}^{N} w_i\varphi_i \epsilon W_h$ for $i = 1, \ldots N$,
   $\Rightarrow a(u_h, \varphi_i) = b(\varphi_i)$, where $i = 1, \ldots N$.
   Using $u_h = \sum_{j=1}^{N} u_j\varphi_j$, for $j = 1, \ldots N$,
   a $(\sum_{i,j=1}^{N} u_j\varphi_j, \varphi_i) = b(\varphi_i)$ for $i, j = 1, 2, 3, \ldots N$,
   $\Rightarrow \sum_{i,j=1}^{N} a(\varphi_j, \varphi_i)u_j = b(\varphi_i)$ for $i, j = 1, 2, 3, \ldots N$.
   where u_j are the solution values at the nodes. Also $a(u, w)$ is bilinear form and $b(w)$ is the linear form.

Example:

Consider a 2D Poisson equation.

$$-\Delta G = f, \quad \text{in} \quad \Omega \tag{2.31}$$

$$G = 0, \quad \text{on} \quad \partial\Omega \tag{2.32}$$

Here, f reprsents the known function and we find G, Ω denotes the domain of problem and $\partial\Omega$ is the boundary of the problem. In order to find the approximate solution of Eq. (2.31) using FEM, the following steps are required:

- Obtain the weak formulation of the Eq. (2.31) as follows

$$-\int_{\Omega} w\Delta G d\Omega = \int_{\Omega} wf d\Omega, \tag{2.33}$$

- Green's theorem is used to get the first order derivatives from second order derivatives.

$$\int_{\Omega} w \frac{\partial G}{\partial n} ds = \int_{\Omega} \nabla w \nabla G d\Omega + \int_{\Omega} w \Delta G d\Omega \tag{2.34}$$

- Substitute Eq. (2.34) into Eq. (2.33), we get

$$-\underbrace{\int_{\Omega} w \frac{\partial G}{\partial n} ds}_{0} + \int_{\Omega} \nabla w \nabla G d\Omega = \int_{\Omega} w f d\Omega, \tag{2.35}$$

the corresponding homogeneous boundary condition is cancelling the boundary integral, so we have

$$\int_{\Omega} \nabla w \nabla G d\Omega = \int_{\Omega} w f d\Omega, \tag{2.36}$$

- Elemental weak form

$$\int_{\Omega_e} \nabla w \nabla G d\Omega = \int_{\Omega^e} w f d\Omega, \tag{2.37}$$

- In 2D cartesian plane, the Eq. (2.37) can be written as,

$$\int_{\Omega_e} \left(\frac{\partial w}{\partial x} \frac{\partial G}{\partial x} + \frac{\partial w}{\partial y} \frac{\partial G}{\partial y} \right) d\Omega = \int_{\Omega^e} w f d\Omega, \tag{2.38}$$

- Over an element the approximate solution is

$$G^e = \sum_{j=1}^{M} G_j^e \zeta_j^e(x, y) \tag{2.39}$$

G_j is the node of solution value and ζ_j is the basis function.

- Assemble local matrices in to the global matrix K and solve the system of equations $KG = F$ to obtain the discrete solution.

Chapter 3

Mixed Convection MHD in Aluminium-Water Nanofluid Filled Porous Cavity

This chapter, we examine the mixed convective magneto-hydrodynamic nanofluid flow in a porous enclosure. The impact of inclined magnetic field and nonlinear thermal radiation is also considered while modeling the momentum and energy equation, respectively. The governing partial differential equations are converted into dimensionless PDEs with the help of appropriate transformation. Galerkin weighted residual method based on finite element technique has been used to solve the considered problem. Influence of the governing parameters is analyzed through isotherms, streamlines and some useful MATLAB graphs. This chapter provides the review of [35].

3.1 The Problem Configuration

We consider the two dimensional square shaped porous enclosure. The schematic diagram of the problem is shown in Figure 3.1. Enclosure is filled with Alumina-water nanofluid. The horizontal walls of the enclosure are maintained at different temperature, the upper surface of the cavity is fixed at cold temperature T_c whereas the bottom surface is maintained at hot temperature T_h. Both the vertical surfaces of the enclosure are adiabatic and they are moving in opposite direction with velocity V_w. The fluid under observation is considered as incompressible and Newtonian. The mixture of base fluid and nanoparticles is stable and having the same temperature. Isotropic and homogenous is considered to be porous medium. Impacts of Joule heating and viscous dissipation are ignored whereas nonlinear thermal radiation has been considered in the energy equation. Thermophysical properties of nanoparticles (Aluminium) and base fluid (water) are considered as constant given in Table 3.1 whereas the density varies with temperature and modeled according to Boussinesq approximation in the momentum equation.

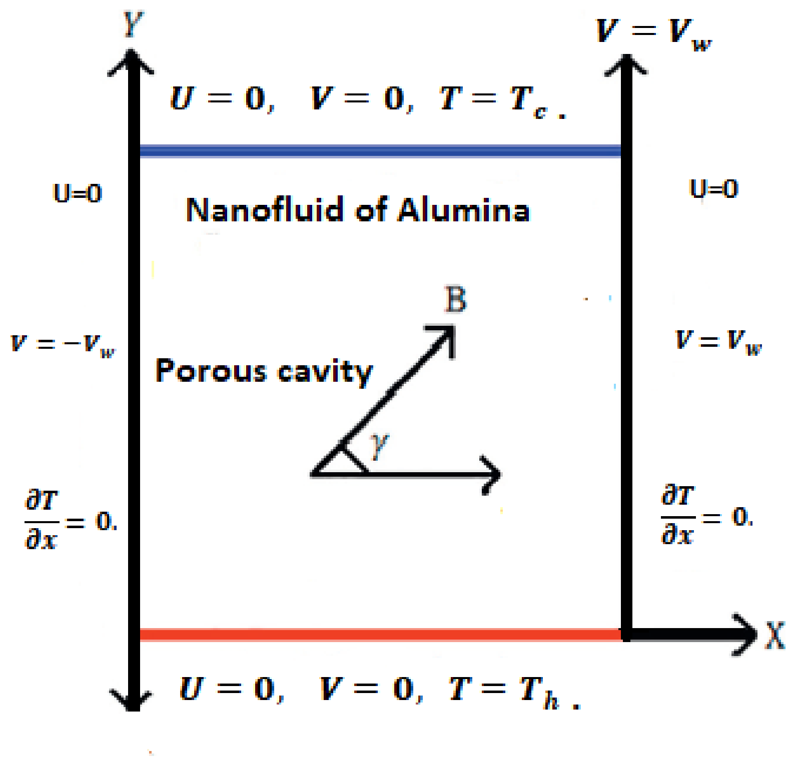

Figure 3.1: Schematic diagram of the physical model.

Physical Properties	H_2O	Al_2O_3
$\rho(\text{kgm}^{-3})$	997.1	3970
$C_p(\text{Jk}g^{-1}\text{K}^{-1})$	4179	765
$k(\text{Wm}^{-1}\text{K}^{-1})$	0.613	40
$\beta(\text{K}^{-1})$	21×10^{-5}	1.89×10^{-5}
$\sigma(\Omega\text{m})^{-1}$	0.05	1×10^{-10}
$d_s(\text{nm})$	-	47

Table 3.1: Thermophysical properties of water (H_2O) and alumina (Al_2O_3).

For nonlinear thermal radiation Rosseland approximation has been adopted [44].

$$q_{rx} = -\frac{4\sigma_*}{3a_*}\frac{\partial T^4}{\partial x} = -\frac{16\sigma_*}{3a_*}T^3\frac{\partial T}{\partial x}, \tag{3.1}$$

$$q_{ry} = -\frac{4\sigma_*}{3a_*}\frac{\partial T^4}{\partial y} = -\frac{16\sigma_*}{3a_*}T^3\frac{\partial T}{\partial y}. \tag{3.2}$$

3.1.1 The Dimensional Governing Equations

The dimensional form of the continuity, momentum and energy equations along with associated boundary conditions for the proposed problem are mentioned below [35]:

Continuity equation:

$$\frac{\partial u}{\partial x} + \frac{\partial v}{\partial y} = 0 \tag{3.3}$$

x and y-momentum equation:

$$\frac{\rho_{nf}}{\epsilon^2}\left(u\frac{\partial u}{\partial x} + v\frac{\partial u}{\partial y}\right) = -\frac{\partial p}{\partial x} + \frac{\mu_{nf}}{\epsilon}\left(\frac{\partial^2 u}{\partial x^2} + \frac{\partial^2 u}{\partial y^2}\right) + \sigma_{nf}B_0^2(v\sin\gamma\cos\gamma - u\sin^2\gamma)$$
$$-\frac{\mu_{nf}}{K}u - \frac{1.75\rho_{nf}}{\sqrt{150K}\epsilon^{\frac{3}{2}}}(\sqrt{u^2+v^2})u. \tag{3.4}$$

$$\frac{\rho_{nf}}{\epsilon^2}\left(u\frac{\partial v}{\partial x} + v\frac{\partial v}{\partial y}\right) = -\frac{\partial p}{\partial y} + \frac{\mu_{nf}}{\epsilon}\left(\frac{\partial^2 v}{\partial x^2} + \frac{\partial^2 v}{\partial y^2}\right) + \sigma_{nf}B_0^2(u\sin\gamma\cos\gamma - v\cos^2\gamma)$$
$$-\frac{\mu_{nf}}{K}v + (\rho\beta)_{nf}g(T - T_c) - \frac{1.75\rho_{nf}}{\sqrt{150K}\epsilon^{\frac{3}{2}}}(\sqrt{u^2+v^2})v. \tag{3.5}$$

Energy equation:

$$u\frac{\partial T}{\partial x} + v\frac{\partial T}{\partial y} = \alpha_{nf}\left(\frac{\partial^2 T}{\partial x^2} + \frac{\partial^2 T}{\partial y^2}\right) - \frac{1}{(\rho C_p)_{nf}}\left(\frac{\partial q_{rx}}{\partial x} + \frac{\partial q_{ry}}{\partial y}\right) \tag{3.6}$$

Dimensional Boundary Conditions

The associated boundary conditions can be given as

- On the upper surface:

$$u = 0, \qquad v = 0, \qquad T = T_c$$

- On the lower surface:

$$u = 0, \qquad v = 0, \qquad T = T_h$$

- On the vertical left surface:

$$u = 0, \qquad v = -V_w, \qquad \frac{\partial T}{\partial x} = 0$$

- On the vertical right surface:

$$u = 0, \qquad v = V_w, \qquad \frac{\partial T}{\partial x} = 0$$

3.1.2 Thermophysical Properties of Nanofluid

The following correlations for the thermophysical properties are considered for the simulation of modeled problem:

- Effective density:

$$\rho_{nf} = (1-\phi)\rho_f + \phi\rho_s.$$

- Thermal diffusivity:

$$\alpha_{nf} = \frac{k_{nf}}{(\rho C_p)_{nf}}.$$

- Specific heat:

$$(\rho C_p)_{nf} = (1-\phi)(\rho C_p)_f + \phi(\rho C_p)_s.$$

- Coefficient of thermal expansion:

$$(\rho\beta)_{nf} = (1-\phi)(\rho\beta)_f + \phi(\rho\beta)_s.$$

- Electrical conductivity:

$$\sigma_{nf} = \sigma_f \left[1 + \frac{3(\sigma-1)\phi}{(\sigma+2)-(\sigma-1)\phi}\right], \sigma = \frac{\sigma_s}{\sigma_f}.$$

- Thermal conductivity:
  The model for effective thermal conductivity was suggested by Koo and Kleinstreuer [45] and is given by

$$k_{nf} = k_{static} + k_{Brownian}.$$

where

$$k_{static} = k_f \left[1 + \frac{3(k_s/k_f-1)\phi}{(k_s/k_f+2)-(k_s/k_f-1)\phi}\right]$$

and

$$k_{Brownian} = 5 \times 10^4 \phi \rho_f (C_p)_f \sqrt{\frac{k_b T}{\rho_s d_s}} g^{'}(T, \phi, d_s).$$

The empirical $g^{'}$-function for Al_2O_3-water nanofluid is written as

$$g^{'}(T,\phi,d_s) = (c_1 + c_2\ln(d_s) + c_3\ln(\phi) + c_4\ln(\phi)\ln(d_s) + c_5\ln{(d_s)^2})\ln(T) \\ + (c_6 + c_7\ln(d_s) + c_8\ln(\phi) + c_9\ln(\phi)\ln(d_s) + c_{10}\ln{(d_s)^2}).$$

Coefficient values	Alumina-water
c_1	52.813488759
c_2	6.115637295
c_3	0.6955745084
c_4	0.041745555278
c_5	0.176919300241
c_6	-298.19819084
c_7	-34.532716906
c_8	-3.9225289283
c_9	-0.2354329626
c_{10}	-0.999063481

Table 3.2: Coefficients for the empherical formula.

- Effective Viscosity:

  Due to micromixing in suspentions, the effective viscosity model was proposed by Koo and Kleinstreuer [46].

$$\mu_{nf} = \mu_{static} + \mu_{Brownian} = \mu_{static} + \frac{k_{Brownian}}{k_f} \times \frac{\mu_f}{Pr_f},$$

  where $\mu_{static} = \mu_f/(1-\phi)^{2.5}$.

- Effective heat capacity due to porosity:

$$(\rho C_p)_m = (1-\epsilon)(\rho C_p)_s + \epsilon(\rho C_p)_{nf}.$$

- Effective thermal conductivity:

$$k_m = (1-\epsilon)k_s + \epsilon k_{nf}.$$

3.1.3 The Non-Dimensional Governing Equations

The following parameters are introduced in order to reduce the governing PDEs to the non-dimensional form.

$$X = \frac{x}{L}, \quad U = \frac{u}{V_w}, \quad Y = \frac{y}{L}, \quad V = \frac{v}{V_w}, \quad P = \frac{p}{\rho_{nf} V_w^2}, \quad \theta = \frac{T - T_c}{T_h - T_c},$$
$$Da = \frac{K}{L^2}, \quad Pr = \frac{\nu_f}{\alpha_f}, \quad Rd = \frac{4\sigma_* T_c^3}{a_* \alpha_f}, \quad Gr = \frac{g\beta \Delta T L^3}{\nu_f^2}, \quad Re = \frac{V_w L}{\nu_f},$$
$$Ha = B_0 L \sqrt{\frac{\sigma_f}{\mu_f}}, \quad Ri = \frac{Gr}{Re^2}, \quad Nr = \frac{T_h}{T_c}.$$

The transformed governing equations are given as

$$\frac{\partial U}{\partial X} + \frac{\partial V}{\partial Y} = 0. \tag{3.7}$$

$$\begin{aligned}\frac{1}{\epsilon^2}\left(U\frac{\partial U}{\partial X} + V\frac{\partial U}{\partial Y}\right) &= -\frac{\partial P}{\partial X} + \frac{1}{\epsilon Re}\frac{\mu_{nf}}{\rho_{nf}\nu_f}\left(\frac{\partial^2 U}{\partial X^2} + \frac{\partial^2 U}{\partial Y^2}\right)\\ &+ \frac{\rho_f}{\rho_{nf}}\frac{\sigma_{nf}}{\sigma_f}\frac{Ha^2}{Re}(V\sin\gamma\cos\gamma - U\sin^2\gamma)\\ &- \frac{\mu_{nf}}{\rho_{nf}\nu_f}\frac{1}{ReDa}U - \frac{1.75}{\sqrt{150Da\epsilon^{\frac{3}{2}}}}(\sqrt{U^2+V^2})U.\end{aligned} \tag{3.8}$$

$$\begin{aligned}\frac{1}{\epsilon^2}\left(U\frac{\partial V}{\partial X} + V\frac{\partial V}{\partial Y}\right) &= -\frac{\partial P}{\partial Y} + \frac{1}{\epsilon Re}\frac{\mu_{nf}}{\rho_{nf}\nu_f}\left(\frac{\partial^2 V}{\partial X^2} + \frac{\partial^2 V}{\partial Y^2}\right)\\ &+ Ri\frac{\rho_f}{\rho_n f}\left(1 - \phi + \frac{\rho_s\beta_s}{\rho_f\beta_f}\phi\right)\theta\\ &+ \frac{\rho_f}{\rho_{nf}}\frac{\sigma_{nf}}{\sigma_f}\frac{Ha^2}{Re}(U\sin\gamma\cos\gamma - V\cos^2\gamma)\\ &- \frac{\mu_{nf}}{\rho_{nf}\nu_f}\frac{1}{ReDa}V - \frac{1.75}{\sqrt{150Da\epsilon^{\frac{3}{2}}}}(\sqrt{U^2+V^2})V.\end{aligned} \tag{3.9}$$

$$U\frac{\partial\theta}{\partial X}+V\frac{\partial\theta}{\partial Y}=\frac{1}{RePr}\left(\frac{\alpha_{nf}}{\alpha_f}\frac{k_m}{k_{nf}}+\frac{4}{3}\frac{Rd}{(\rho C_p)_{nf}}(1+(Nr-1)\theta)^3\right)\left(\frac{\partial^2\theta}{\partial X^2}+\frac{\partial^2\theta}{\partial Y^2}\right) \tag{3.10}$$

Dimensionless Boundary Conditions:

The dimensionless boundary conditions implemented for the model problem are reduced as:

- On the upper surface:

$$U = 0, \qquad V = 0, \qquad \theta = 0.$$

- On the lower surface:

$$U = 0, \qquad V = 0, \qquad \theta = 1.$$

- On the left vertical surface:

$$U = 0, \qquad V = -1, \qquad \frac{\partial\theta}{\partial X} = 0.$$

- On the right vertical surface:

$$U = 0, \qquad V = 1, \qquad \frac{\partial\theta}{\partial X} = 0.$$

3.1.4 The Nusselt Number

The local Nu and Nu_{avg} at the hot lower surface are as follows:

$Nu=-\frac{k_{nf}}{k_f}(1+\frac{4}{3}RdNr^3)\left(\frac{\partial\theta}{\partial Y}\right)|_{Y=0}$

$Nu_{avg}=\int_0^1 NudX$

3.2 The Numerical Solution

The Galerkin based finite element method is applied to find the numerical solution of the governing system of partial differential equations for the velocity, pressure and temperature components. The dimensionless governing partial differential equations are first transformed into weak or variational form by multiplying the suitable test function and integrating over the computational domain. In particular, the discretization of the equations is performed with the help of higher order Ladyzhenskaya-Babuska-Brezzi (LBB) stable Q_2/P_1^{disc} -element pair (see for [47] for further details). That means the biquadratic (Q_2) finite element space is utilized for the velocity components, temperature and pressure is approximated in the linear discontinuous (P_1^{disc}) finite element space. After that the integration on each term is carried out by using the appropriate Gaussian quadrature method. The biquadratic element (Q_2) has 9 local unknowns for each velocity and temperature variables and 3 unknowns for the piecewise linear (P_1^{disc}) pressure in each element. Thus, a total of 30 unknowns for each element consisting of velocity, pressure and temperature components needs to be computed. It is considered the sequences of structured nodes, which are generated through uniform refinement from a coarsest grid ($l = 1$) having one element only. A regular refinement constructs the mesh of any higher level ($l + 1$) by joining the opposite mid points of element edges (see [48, 49] for further details). Figure 3.2 depicts the grids for various levels $\ell = 1, 2, 3$, respectively. The discretized systems of nonlinear algebraic equations are computed with the help of Newton's method and the linearized subproblems in each nonlinear iteration are solved by using the Gaussian elimination method. The convergence is achieved by making sure that nonlinear residual falls below 10^{-6} in the l^2-norm. First, we take coarsest mesh containing one cell only at level $\ell = 1$ then it is refined by sequence of meshes for next higher levels, i.e., $\ell + 1$ (see Figure 3.2).

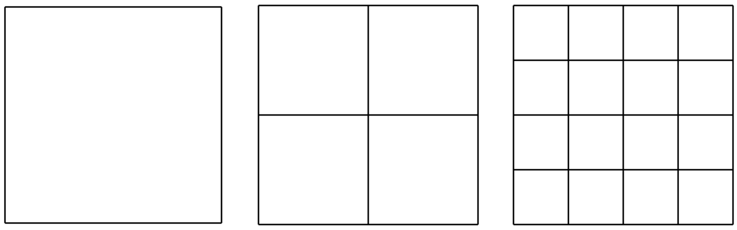

Figure 3.2: The sequence of grids on space mesh level = 1,2,3 (from left to right).

3.2.1 The Code Validation

The given Table 3.3 shows the code validation for the mixed convection flow where it can be seen that results have good agreement with published results in the literature. Table 3.4 shows the grid convergence test for different computation levels for Nu_{avg} with $\gamma = 0$, $\epsilon = 0.6$, Nr=1.1, Ri=(1 and 10), Re=100, $Da = 10^{-3}$, $\phi = 0.04$, Ha=25 and Rd=1. The number of elements (#EL)and total number of degree of freedom (#DOFs) which are essential for the approximation of temperature, velocity and pressure with respect to used discretization are shown in Table 3.4. First, the coarsest grid comprising of only one element at level ℓ=1, then the level $\ell = \ell + 1$ is acquired by dividing each of the element in to four elements by joinning midpoints of opposite faces.

Reynolds Number	Present Study	Ref. [50]	Ref. [51]	Ref. [52]	Ref. [53]	Ref. [54]	Ref. [55]
100	2.03	2.05	2.01	-	2.09	-	1.94
400	4.02	4.09	3.97	4.14	4.16	4.05	3.84
1000	6.40	6.70	6.28	6.61	6.55	6.55	6.33

Table 3.3: Comparison of present results for Nu_{avg} with those of [68-73] for Gr=100.

ℓ	# EL	# DOFs	$Nu_{avg}(Ri = 1)$
4	64	1059	3.873425
5	256	4035	3.562933
6	1024	15,747	3.162628
7	4096	62,211	2.951288
8	16,384	247,299	2.848920

Table 3.4: The grid independence results for alumina-water nanofluid.

3.3 Results and Discussion

Numerical results are obtained for the mixed convection of alumina-water nanofluid considering the impact of inclined magnetic field and nonlinear thermal radiation for various governing parameters. The standard variables are taken as $\phi = 0.04$, $Ri = 1$, $\gamma = 0$, $Nr = 1.1$, $Rd = 1$, $Re = 100$, $\epsilon = 0.6$, $Da = 10^{-3}$, $Ha = 25$ unless they are mentioned in the entire study.

Figure 3.3 explains the influence of radiation parameter on streamlines for $Ri = 0.01$, 1 and 10. For small value of Richardson number $Ri = 0.01$ the streamlines show the similar behaviour as $Ri = 1$. For these values, the weak eddies are observed near the vertical walls of the cavity. The deeper flow activity is noticed due to enhancement of buoyancy forces with augumentation of the Ri up to 10 and hence the respective changes in flow behaviour are observed. As a result weak vortices are combined into a single strong vortex in the middle of the enclosure. This shows that the fluid has heigher velocity in this case.

Figure 3.4 demonstrates the impact of radiation parameter on isotherms for Ri at 0.01, 1 and 10. For small values of $Ri = 0.01$ and 1, the isotherms show almost the similar pattern as in the case of streamlines. On the right lower corner of cavity isotherms with large magnitude are observed while low magnitude isotherms are being observed in the upper left corner.For the value of $Rd = 3$, isotherms are moving obliquely from left lower to upper right corner of the enclosure. The isothermal lines are equally spreaded as the Rd increases up to 5. This indicates that conduction is leading in the enclosure.

Figure 3.5 and 3.6 show the influence of porosity parameter on the streamlines amd isotherms respectively for the values of $Ri = 0.01$, 1 and 10. Mainly, the two weak vortices along the opposite vertical adiabatic surfaces for $\epsilon = 0.2$ and $Ri = 0.01$, 1, are being observed in Figure 3.5. The eddies become strong and maximum for $\epsilon = 0.8$ as porosity parameter increases which is also obvious from the maximum value of stream function.

As the porosity values changes from lower value to higher value, the isothermal lines show higher movement from upper left corner towards lower right corner. It means with increase in the porosity, we observe the maximum growth of isotherms. For different value of porosity parameter used for $Ri = 0.01$ and $Ri = 1$, there exist very less variation in isothermal patterns but significant variations occur for $Ri = 10$. The gradual increase in porosity values for $Ri = 10$ show the gradual conversion of conduction to convection in flow behaviour.

Figure 3.7 illustrate the influence of thermal radiation parameter on the average Nu for all three regimes of convection. The average Nu is linearly increasing with the augmentation of Rd.

Figure 3.8 shows that the effect of Rd on θ_{avg} for different values of Ri. The rate of heat transfer is increased for all the case of convection, whereas θ_{avg} is increased with radiation parameter and having same trends for all the values of Richardson number.

Figure 3.9 demonstrates the impact of temperature ratio parameter on the Nu_{avg} for different values of Richardson number that is 0.01, 1 and 10. Average Nusselt number having direct relation with temperature ratio parameter. It can be noticed that more heat is transfered in case of $Ri = 10$ act as compared to $Ri = 0.01$ which shows that the moving surface is responsible for the heat transfer in all over the cavity.

Figure 3.10 illuminates the effect of temperature ratio parameter (Nr) on average temperature for all values of convection. Increasing the values of Nr enhances the thermal state of fluid which is responsible for enhancement of average temperature, whereas θ_{avg} is reducing for modes of convection which shows that forced convection is leading over the free convection and all of the heat is transferred through bottom hot wall.

Figure 3.11 depicts that the behaviour of Nu_{avg} in porosity parameter. It means an increasing value of porosity parameter for $Ri = 10$ we get maximum value of Nu_{avg}.This shows that the increase in heat transfer is more prominent for free convection in flow regime for $Ri = 10$.

Figure 3.12 displays that the temperature is enhanced with the increasing values of porosity parameter. Again increasing value of $Ri = 10$ shows decreasing effects on the value of θ_{avg}.

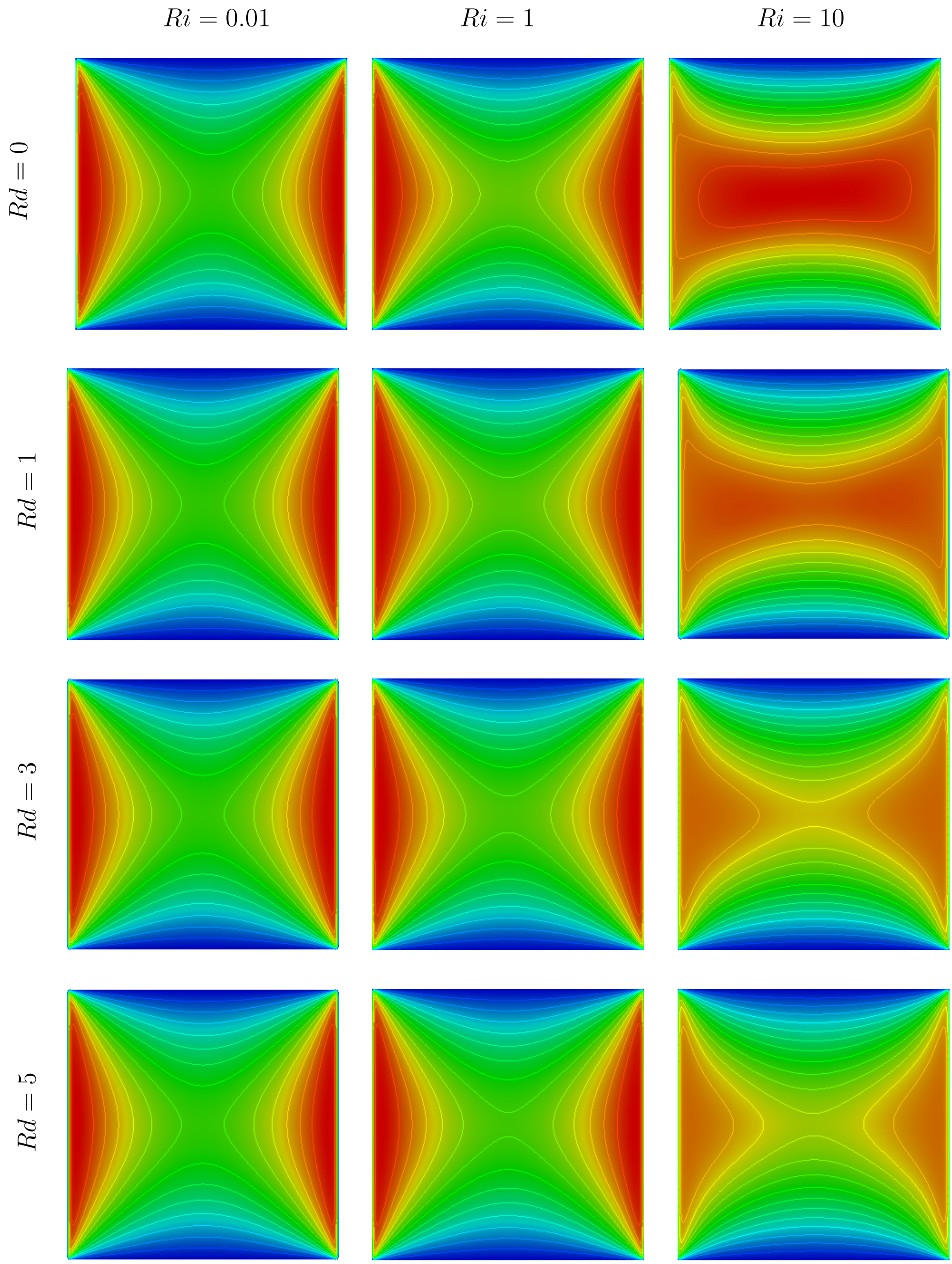

Figure 3.3: Streamlines for different values of Rd with $\epsilon = 0.6$, $\phi = 0.04$, $Ha = 25$, $\gamma = 0$, $Re = 100$, $Nr = 1.1$, and $Da = 10^{-3}$.

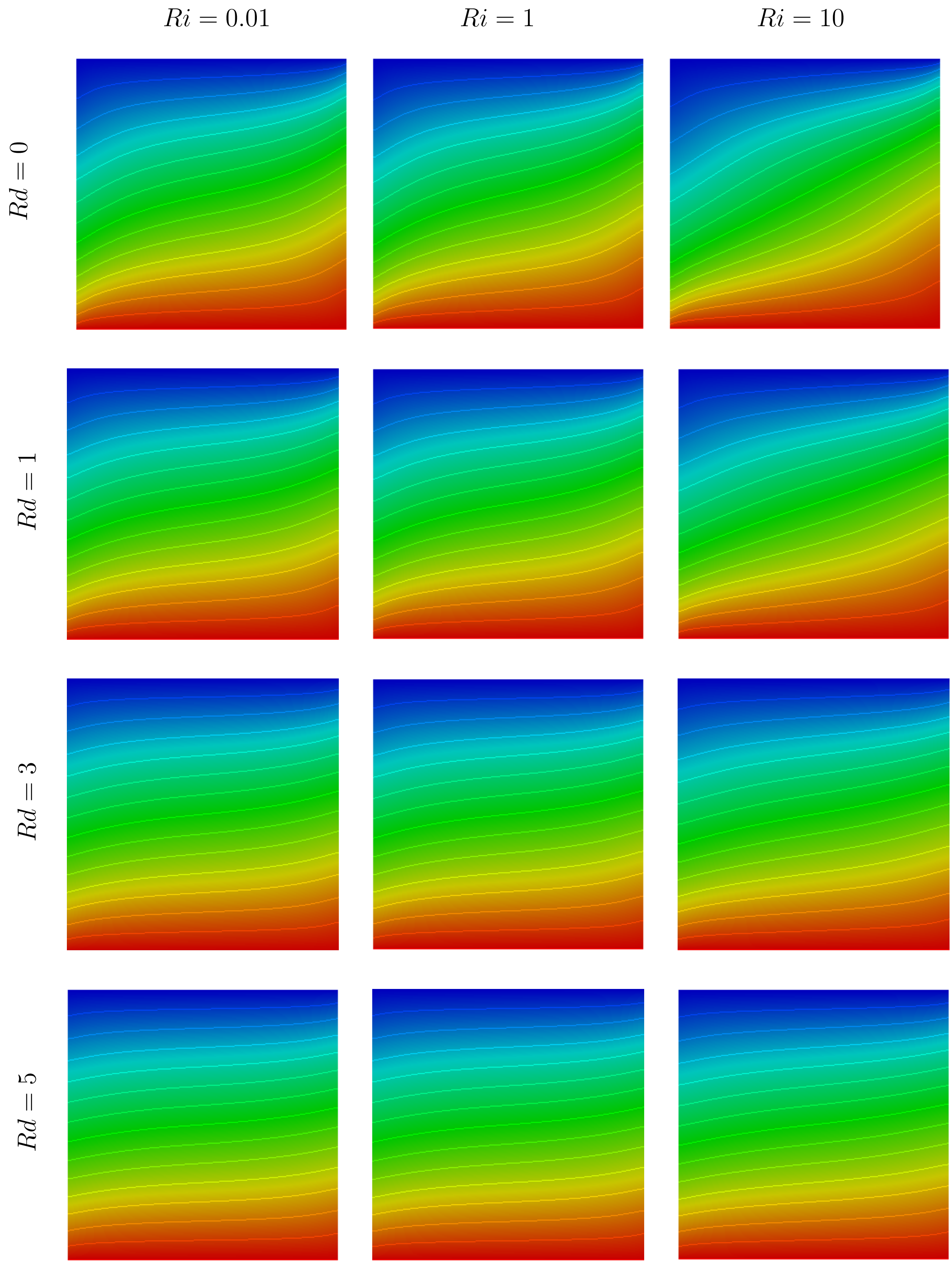

Figure 3.4: Isotherms shapes for different Rd with $\gamma = 0$, $Nr = 1.1$, $\epsilon = 0.6$, $Da = 10^{-3}$,$\phi = 0.04$, $Re = 100$, and $Ha = 25$.

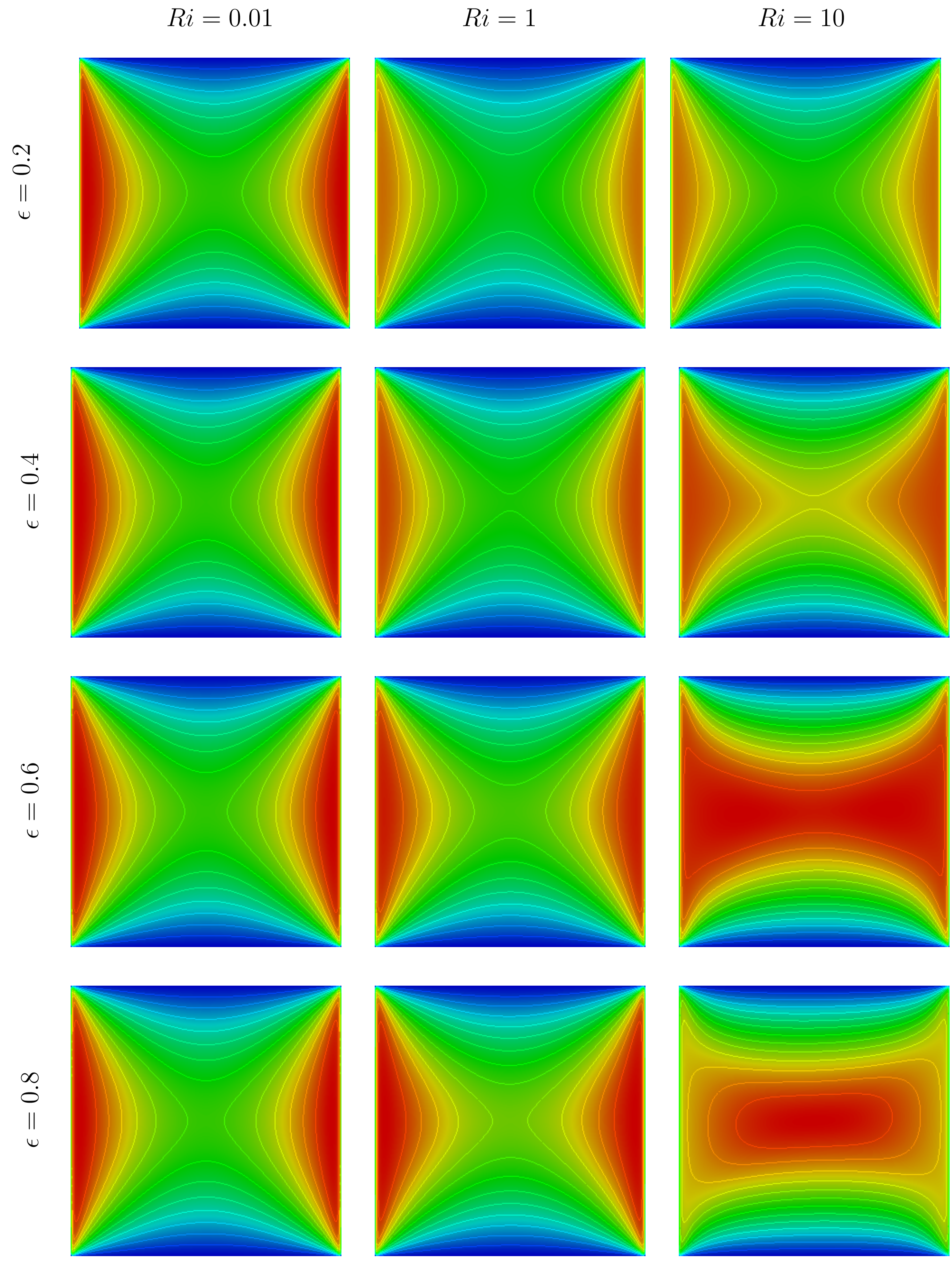

Figure 3.5: Streamlines contours for different ϵ with $\gamma = 0$, $Rd = 1.0$, $\phi = 0.04$, $Nr = 1.1$, $Re = 100$, $Da = 10^{-3}$ and $Ha = 25$.

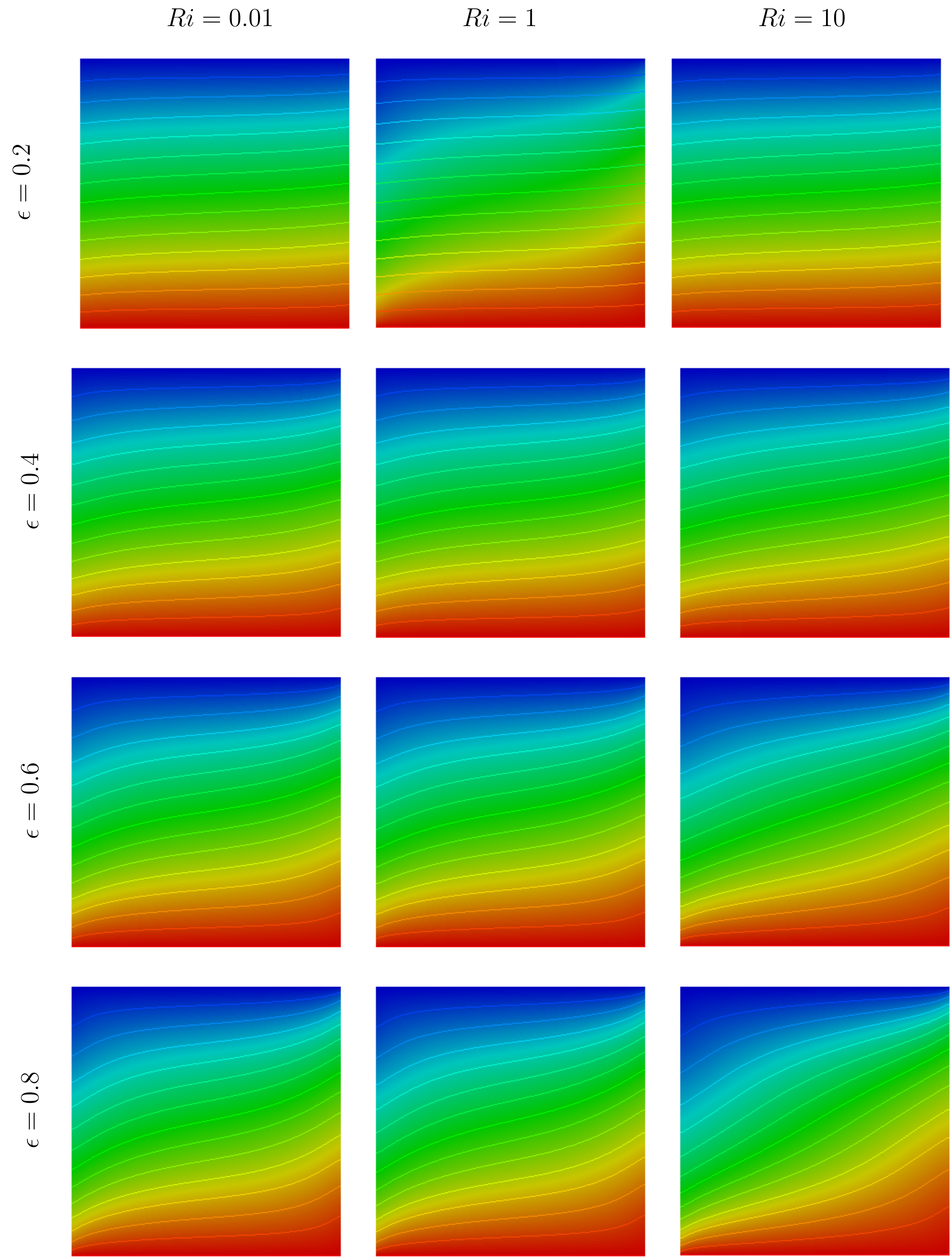

Figure 3.6: Isotherms contours for different ϵ with $Rd = 1.0$, $\gamma = 0$, $Nr = 1.1$, $Da = 10^{-3}$, $Ha = 25$, $\phi = 0.04$ and $Re = 100$.

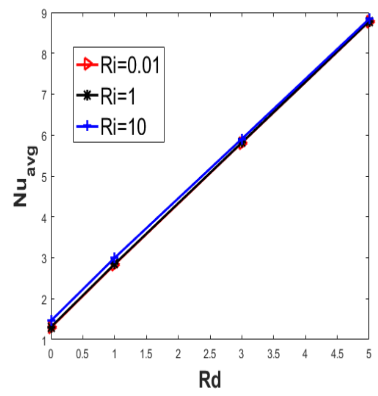

Figure 3.7: Effect of Ri on Nu_{avg} at the bottom hot surface due to Rd.

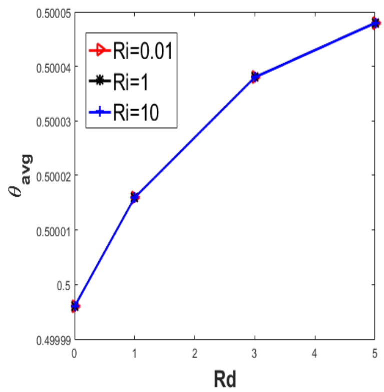

Figure 3.8: Effect of Ri on θ_{avg} as a function of radiation parameter.

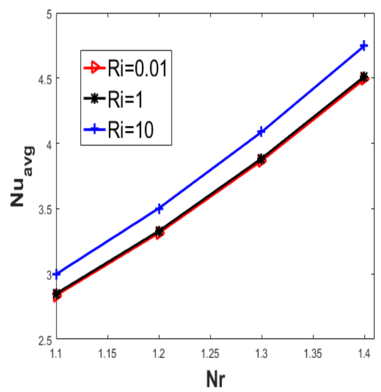

Figure 3.9: Effect of Ri on Nu_{avg} at the bottom hot surface due to Nr.

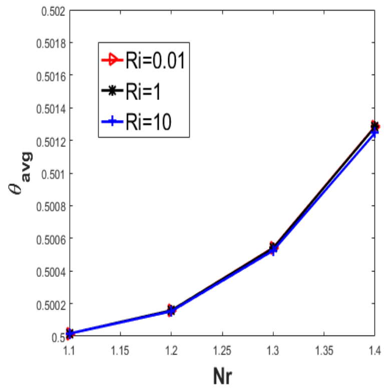

Figure 3.10: Effect of Ri on θ_{avg} as a function of temperature ratio parameter.

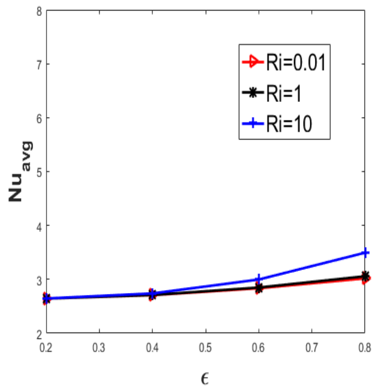

Figure 3.11: Effect of Ri on Nu_{avg} at the bottom hot surface due to ϵ.

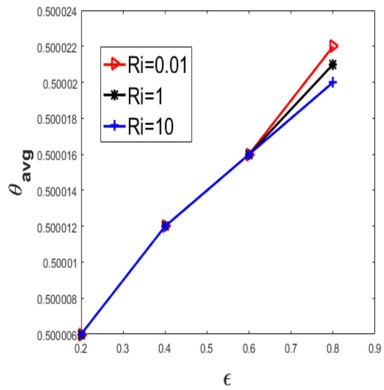

Figure 3.12: Effect of Ri on θ_{avg} as a function of porosity parameter.

Chapter 4

MHD and Joule Heating Impact in Porous Cavity Filled with Nanofluid

The main aim of this chapter is to extend the work of Mehmood *et al.* [35] and analyze the impact of Joule heating numerically through streamlines, isotherms and useful MATLAB graphs. The non-dimensional governing equations are solved using the stable finite pair Q_2/P_1^{disc}.

4.1 Problem Formulation

The system to be examined is a two dimensional, Newtonian, incompressible flow in lid-driven porous square cavity having nanofluid considering the effect of Joule heating. The upper wall and lower wall of the cavity has been reserved at cold temperature T_c and hot temperature T_h, respectively, where as both vertical surfaces are moving with velocity V_w in opposite directions and are adiabatic. The internal heat generation, viscous dissipation and slipping effect between any two phases in the energy equation are ignored. In the present study we considered the

Joule heating in the modeling of energy equation. Physical situation along with boundary conditions of proposed system has been shown in Figure 3.1.

4.1.1 The Dimensional Governing Equations

The governing PDEs and boundary conditionsunder the above described suppositions are as:

Continuity equation:

$$\frac{\partial u}{\partial x} + \frac{\partial v}{\partial y} = 0 \tag{4.1}$$

x-momentum equation:

$$\begin{aligned}\frac{\rho_{nf}}{\epsilon^2}\left(u\frac{\partial u}{\partial x} + v\frac{\partial u}{\partial y}\right) = -\frac{\partial p}{\partial x} + \frac{\mu_{nf}}{\epsilon}\left(\frac{\partial^2 u}{\partial x^2} + \frac{\partial^2 u}{\partial y^2}\right) + \sigma_{nf}B_0^2(v\sin\gamma\cos\gamma - u\sin^2\gamma)\\ - \frac{\mu_{nf}}{K}u - \frac{1.75\rho_{nf}}{\sqrt{150K}\epsilon^{\frac{3}{2}}}(\sqrt{u^2+v^2})u.\end{aligned} \tag{4.2}$$

y-momentum equation:

$$\begin{aligned}\frac{\rho_{nf}}{\epsilon^2}\left(u\frac{\partial v}{\partial x} + v\frac{\partial v}{\partial y}\right) = -\frac{\partial p}{\partial y} + \frac{\mu_{nf}}{\epsilon}\left(\frac{\partial^2 v}{\partial x^2} + \frac{\partial^2 v}{\partial y^2}\right) + \sigma_{nf}B_0^2(u\sin\gamma\cos\gamma - v\cos^2\gamma)\\ - \frac{\mu_{nf}}{K}v + (\rho\beta)_{nf}g(T-T_c) - \frac{1.75\rho_{nf}}{\sqrt{150K}\epsilon^{\frac{3}{2}}}(\sqrt{u^2+v^2})v.\end{aligned} \tag{4.3}$$

Energy equation:

$$\begin{aligned}u\frac{\partial T}{\partial x} + v\frac{\partial T}{\partial y} = \alpha_{nf}\left(\frac{\partial^2 T}{\partial x^2} + \frac{\partial^2 T}{\partial y^2}\right) - \frac{1}{(\rho C_p)_{nf}}\left(\frac{\partial q_{rx}}{\partial x} + \frac{\partial q_{ry}}{\partial y}\right)\\ + \frac{\sigma_{nf}}{(\rho C_p)_{nf}}B_0^2 v^2.\end{aligned} \tag{4.4}$$

Here u, v represent the components of velocity along x and y-axis respectively, C_p denote specific heat, ρ is the fluid density and B_0 is magnetic field strength.

Dimensional Boundary Conditions

The boundary conditions of the proposed problem are described below:

- On the upper edge:

$$u = 0, \qquad v = 0, \qquad T = T_c$$

- On the lower edge:

$$u = 0, \qquad v = 0, \qquad T = T_h$$

- On the vertical left edge:

$$u = 0, \qquad v = -V_w, \qquad \frac{\partial T}{\partial x} = 0$$

- On the vertical right edge:

$$u = 0, \qquad v = V_w, \qquad \frac{\partial T}{\partial x} = 0$$

4.1.2 Non-Dimensional Form of the Governing Equations

The above governing Equations (4.1) - (4.4) are reduced into non-dimensional form with the help of following parameters:

$$X = \frac{x}{L}, \quad Y = \frac{y}{L}, \quad U = \frac{u}{V_w}, \quad V = \frac{v}{V_w}, \quad \theta = \frac{T - T_c}{T_h - T_c}, \quad P = \frac{p}{\rho_{nf} V_w^2},$$

$$Da = \frac{K}{L^2}, \quad Rd = \frac{4\sigma_* T_c^3}{a_* \alpha_f}, \quad Re = \frac{V_w L}{\nu_f}, \quad Gr = \frac{g\beta \Delta T L^3}{\nu_f^2}, \quad Pr = \frac{\nu_f}{\alpha_f},$$

$$Ha = B_0 L \sqrt{\frac{\sigma_f}{\mu_f}}, \quad Ri = \frac{Gr}{Re^2}, \quad Nr = \frac{T_h}{T_c}, \quad Ec = \frac{V_w^2}{(\rho Cp)_f (T_h - T_c)} \text{(Eckert number)}.$$

$$\frac{\partial U}{\partial X}+\frac{\partial V}{\partial Y}=0. \tag{4.5}$$

$$\begin{aligned}\frac{1}{\epsilon^2}\left(U\frac{\partial U}{\partial X}+V\frac{\partial U}{\partial Y}\right)&=-\frac{\partial P}{\partial X}+\frac{1}{\epsilon Re}\frac{\mu_{nf}}{\rho_{nf}\nu_f}\left(\frac{\partial^2 U}{\partial X^2}+\frac{\partial^2 U}{\partial Y^2}\right)\\&+\frac{\rho_f}{\rho_{nf}}\frac{\sigma_{nf}}{\sigma_f}\frac{Ha^2}{Re}(V\sin\gamma\cos\gamma-U\sin^2\gamma)\\&-\frac{\mu_{nf}}{\rho_{nf}\nu_f}\frac{1}{ReDa}U-\frac{1.75}{\sqrt{150Da}\epsilon^{\frac{3}{2}}}(\sqrt{U^2+V^2})U.\end{aligned} \tag{4.6}$$

$$\begin{aligned}\frac{1}{\epsilon^2}\left(U\frac{\partial V}{\partial X}+V\frac{\partial V}{\partial Y}\right)&=-\frac{\partial P}{\partial Y}+\frac{1}{\epsilon Re}\frac{\mu_{nf}}{\rho_{nf}\nu_f}\left(\frac{\partial^2 V}{\partial X^2}+\frac{\partial^2 V}{\partial Y^2}\right)\\&+Ri\frac{\rho_f}{\rho_n f}\left(1-\phi+\frac{\rho_s\beta_s}{\rho_f\beta_f}\phi\right)\theta\\&+\frac{\rho_f}{\rho_{nf}}\frac{\sigma_{nf}}{\sigma_f}\frac{Ha^2}{Re}(U\sin\gamma\cos\gamma-V\cos^2\gamma)-\frac{\mu_{nf}}{\rho_{nf}\nu_f}\frac{1}{ReDa}V\\&-\frac{1.75}{\sqrt{150Da}\epsilon^{\frac{3}{2}}}(\sqrt{U^2+V^2})V.\end{aligned} \tag{4.7}$$

$$\begin{aligned}U\frac{\partial\theta}{\partial X}+V\frac{\partial\theta}{\partial Y}&=\frac{1}{RePr}\left(\frac{\alpha_{nf}}{\alpha_f}\frac{k_m}{k_{nf}}+\frac{4}{3}\frac{Rd}{(\rho C_p)_{nf}}(1+(Nr-1)\theta)^3\right)\\&\left(\frac{\partial^2\theta}{\partial X^2}+\frac{\partial^2\theta}{\partial Y^2}\right)+\frac{Ha^2Ec}{Re}\frac{\sigma_{nf}}{\sigma_f}\frac{(\rho C_p)_f}{(\rho C_p)_{nf}}V^2.\end{aligned} \tag{4.8}$$

The Dimensionless Boundary Conditions

The dimensionless boundary condition for each wall of enclosure are written below:

- On the upper edge:

$$U\ =\ 0,\qquad V\ =\ 0,\qquad \theta\ =\ 0$$

- On the lower edge:

$$U\ =\ 0,\qquad V\ =\ 0,\qquad \theta\ =\ 1$$

- On the vertical left edge:

$$U = 0, \qquad V = -1, \qquad \frac{\partial \theta}{\partial X} = 0$$

- On the vertical right edge:

$$U = 0, \qquad V = 1, \qquad \frac{\partial \theta}{\partial X} = 0$$

4.2 Results and Discussion

Mixed convection magneto-hydrodynamic in porous enclosure filled with alumina-water nanofluid considering the impact of inclined magnetic field, Joule heating and non-linear thermal radiation is analyzed for various governing parameters. In overall study the standard physical parameters (Rd=1, Re=100, Ha=25, ϵ=0.6, Nr=1.1, ϕ=0.04, $Ec = 10^{-4}$, γ=0, Ri=1 and $Da = 10^{-3}$) have been taken unless they are mentioned. The governing Equations (4.1) - (4.4) are solved using the FEM explained in Chapter 3 including the effect of Joule heating.

Figure 4.1 exhibits the impact of Hartmann number on streamlines for $Ri = 0.01$, 1 and 10. For the values of $Ha = 0$, $Ri = 0.01$ and 1, the two parabolic shaped rotational vortices seem near the vertical surfaces primarily due to their movement in the different ways. Furthermore, increase in Hartmman number up to $Ha = 100$ for the case of $Ri = 10$ exibits that two rotating vortices nearby the vertical surfaces are ultimately combined into a central main vertex in the center of the enclosure. Figure 4.2 displays the effect of Hartmman number on isotherms for different modes of convection $Ri =$ 0.01, 1 and 10. The isotherms display the similar behaviour for small values of Ri. For small Hartmann number, the greater lines for isotherms appear at the right and small lines for isotherms occurs at the left corner of the enclosure. The isotherms appear to travel diagonally from left lower to upper right vortex of the enclosure.

Figure 4.3 is illuminating the influence of Eckert number on streamlines for $Ri = 0.01$, 1 and 10. The similar pattern for the values of $Ri = 0.01$ and 1 is shown on the streamlines, for these values the two weak eddies are observed at vertical surfaces of the cavity. The flow deeper activity in the enclosure is induced with an increase in Ri up to 10.The maximum stream function value increases when Eckert parameter is progressively increases from $Ec = 0$ to $Ec = 10^{-4}$and it is more marked for the case of $Ri = 10$. In this state, weak rotating vortices ultimately merge into a single eddy in the center of the enclosure demonstrating higher fluid velocity. Figure 4.4 shows the impact of Eckert number on isotherms contours for different modes of convection $Ri = 0.01$, 1 and 10. The Eckert number changes from lower to higher value, it results in maximum value of stream function. For different values of Eckert number used for Ri= 0.01 and 1, there exit very less variation in isothermal patterns but significant variation occur for $Ri = 10$.

Figure 4.5 and Figure 4.6 illustrate the effect of Hartmann number on average Nu and average temperature for all the regimes of convection. Nusselt number is declined by increasing the Ha due to Lorentz force produced in the cavity while average Nu is enhanced with the increment of Richardson number. For $Ri = 10$ after some value reduction has been noticed. It means conduction is more effective for the heat transfer. For temperature profile, Ha has direct relation with θ_{avg} for all the case of convection.

Figure 4.7 and Figure 4.8 display the impact of Eckert number on Nu_{avg} and θ_{avg} for all different modes of Richardson number such that $Ri = 0.01$, 1 and 10. As Ec represents the Joule heating effect which resists the rate of heat transfer in the enclosure, so with enhancing the Ec average Nu is linearly decreasing and average temperature linearly increasing for all the values of Ri. It shows that due to high resistance temperature gradient enhancing whereas Nu is falling in the cavity.

Figure 4.9 and Figure 4.10 illuminate the effect of Reynolds number on average Nu and θ_{avg} for all the modes of convection. Enhancement in Re rate of heat transfer increases which is more pronounced in case of $Ri = 10$ while opposite trend observed for temperature gradient.

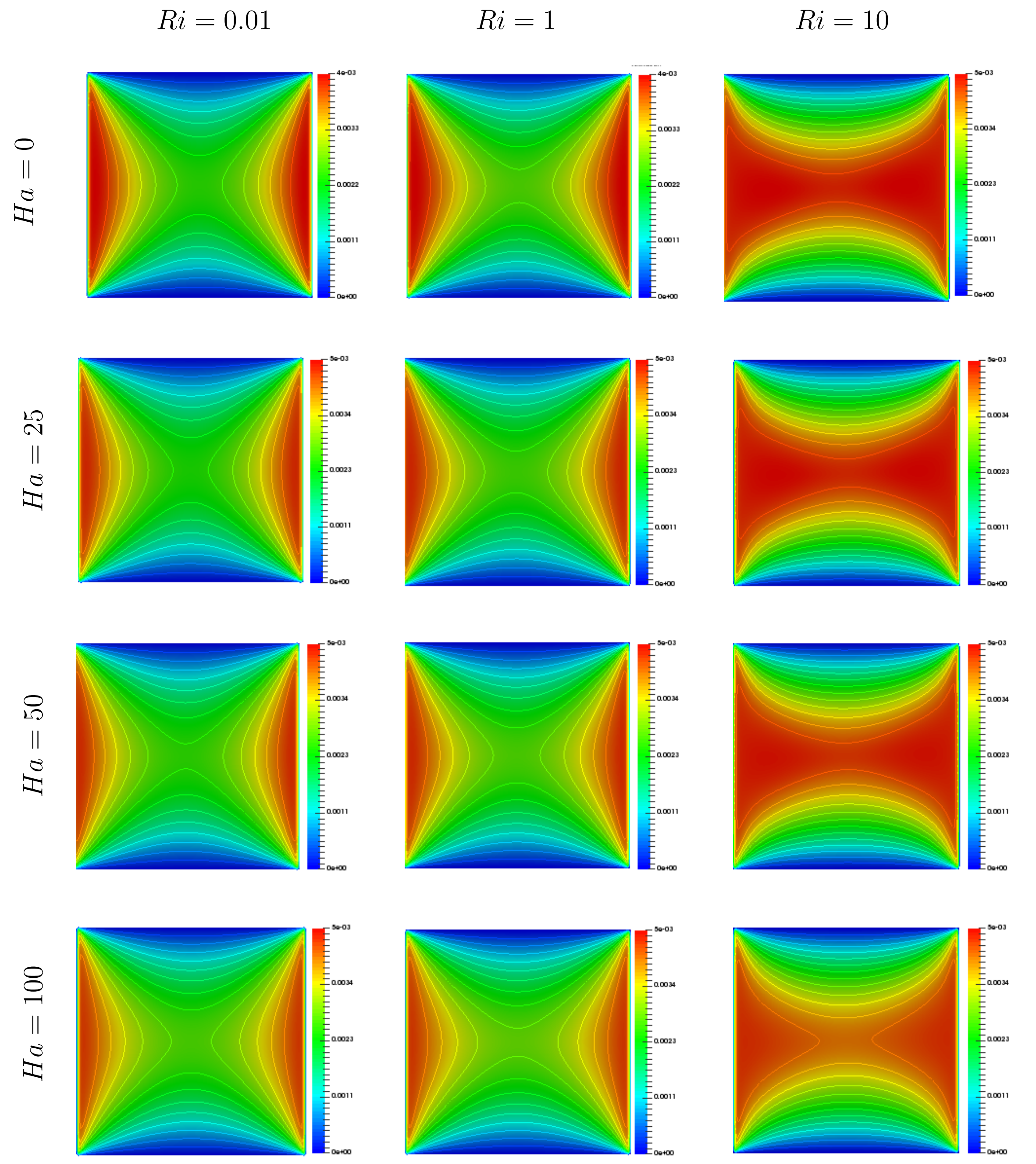

Figure 4.1: Streamlines contours for different Ha with $\gamma = 0$, $\phi = 0.04$, $\epsilon = 0.6$, $Nr = 1.1$, $Rd = 1$, $Ec = 10^{-4}$, $Da = 10^{-3}$ and $Re = 100$,.

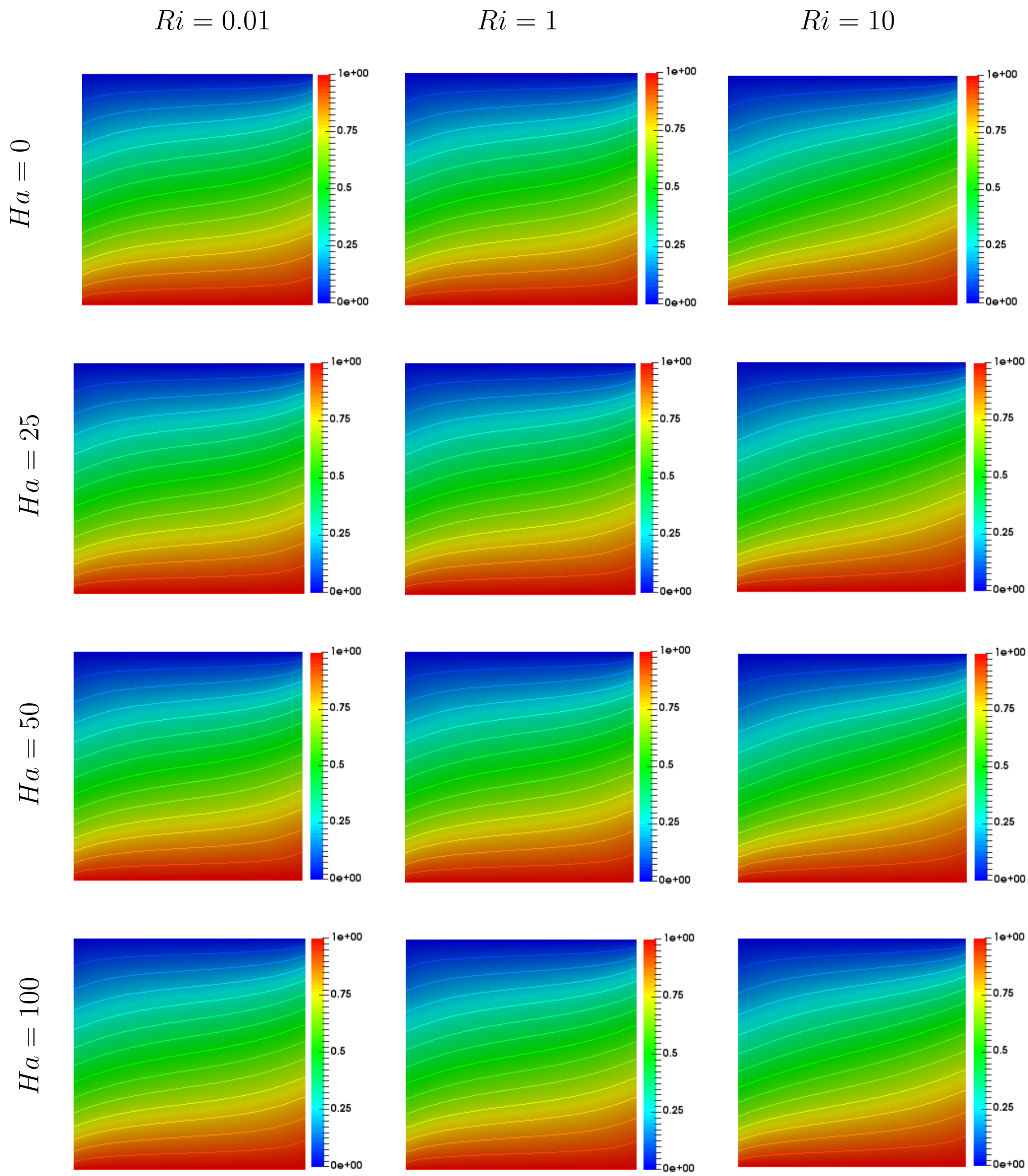

Figure 4.2: Isotherms profiles for different Hartmann number with $Nr = 1.1$, $\phi = 0.04$, $Re = 100$, $Da = 10^{-3}$, $\epsilon = 0.6$, $Rd = 1$, $Ec = 10^{-4}$ and $\gamma = 0$.

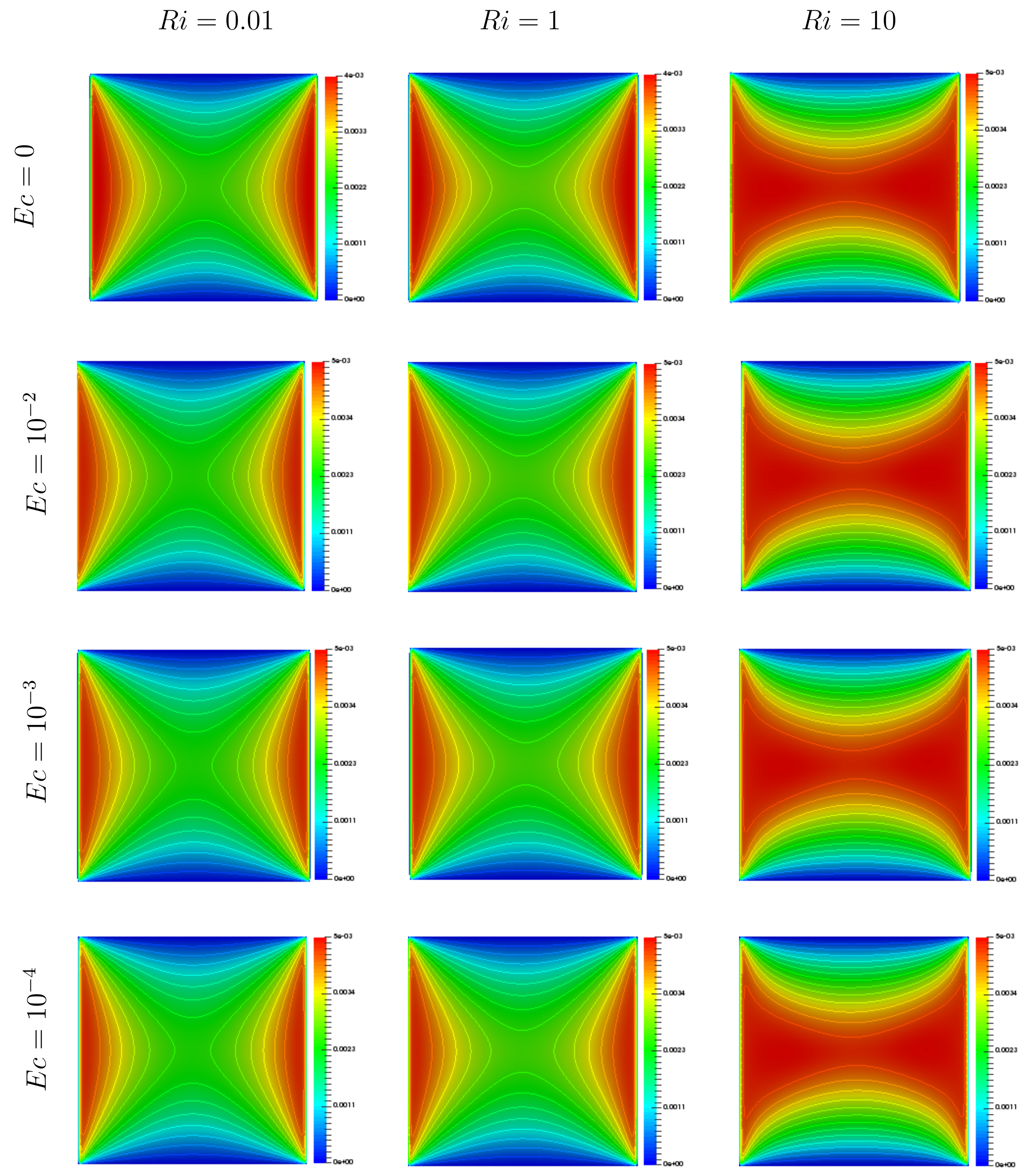

Figure 4.3: Streamlines contours for different Eckert number with $\gamma = 0$ $Ha = 25$, $Nr = 1.1$, $\phi = 0.04$, $\epsilon = 0.6$, $Rd = 1$,$Re = 100$ and $Da = 10^{-3}$.

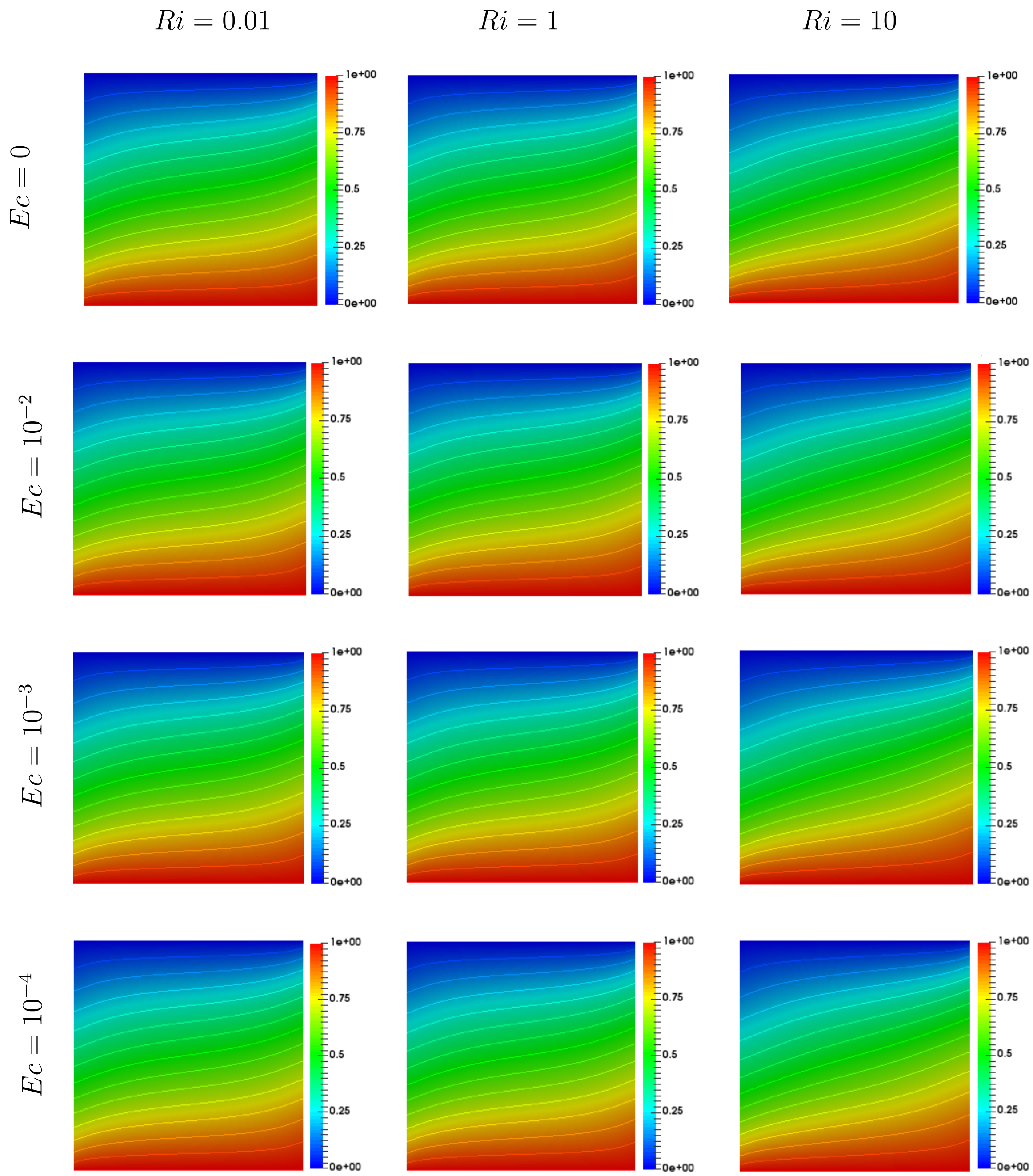

Figure 4.4: Isotherms for different Eckert number with $Ha = 25$, $\phi = 0.04$, $\gamma = 0$, $Da = 10^{-3}$, $Nr = 1.1$, $\epsilon = 0.6$, $Rd = 1$ and $Re = 100$.

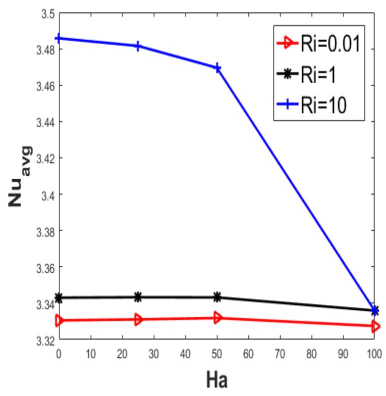

Figure 4.5: Impact of Ri on Nu_{avg} as different values of Ha.

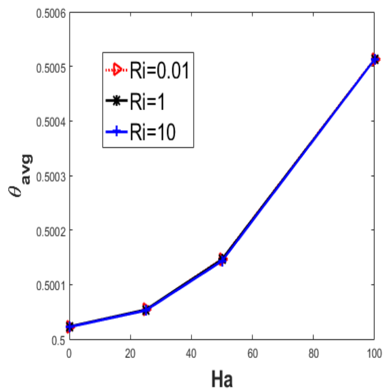

Figure 4.6: Effect of Ri on θ_{avg} as a function of Ha.

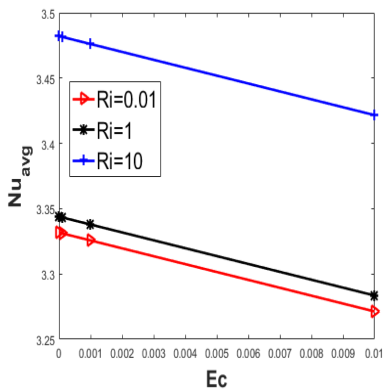

Figure 4.7: Impact of Ri on Nu_{avg} as different modes of Ec.

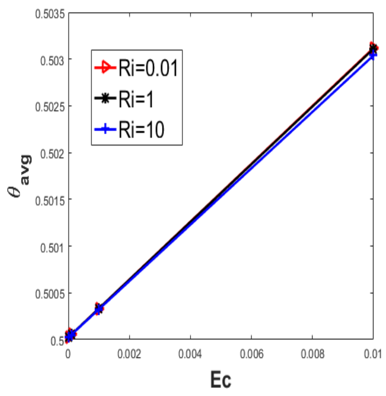

Figure 4.8: Effect of Ri on θ_{avg} as a function of Ec.

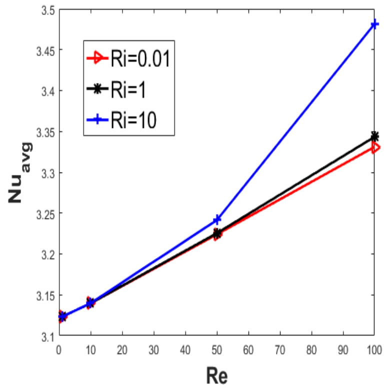

Figure 4.9: Impact of Ri on Nu_{avg} as a function of Re.

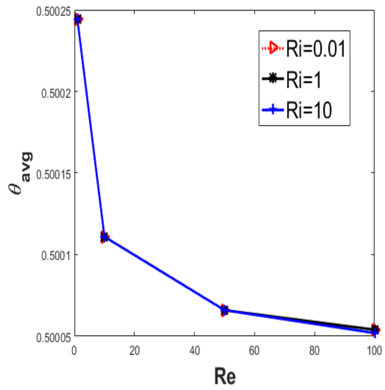

Figure 4.10: Effect of Ri on θ_{avg} as a function of Re.

Chapter 5

Conclusion and Future Work

5.1 Conclusion

In the present work, a steady and two dimensional incompressible mixed convection MHD flow in a porous enclosure thermal radiation together with Joule heating is analyzed. The lower hot wall of the enclosure having a temperature T_h and the upper surface of the enclosure is kept at the cold temperature T_c. On the other hand, the vertical surfaces are moving with velocity V_w in different directions and kept adiabetic. The flow is smooth and stable in nature. P_1^{disc} element of 2nd order accuracy is used to estimate the pressure and Q_2-element of 3rd order accuracy is employed for the discretization of velocity component and temperature. In the entire study the pertinent parameters the Richardson number, Darcy number, porosity parameter, Eckert number, Hartmann number, temperature ratio parameter and Reynolds number. The impacts of governing parameters on dimensionless temperature and velocity are examined with the help of streamlines, graphs and isotherms.

In addition to the review work of Mehmood *et al.* [35], we examined the work for effect of Joule heating in the energy equation. By the GFEM, the governing equations have been solved. The impact of Eckert number, Hartmann number and Reynolds number have been studied through isotherms and streamlines. The

Nu_{avg} and θ_{avg} are examined and plotted for the values of various parameters by using MATLAB. We have numerically analyzed the following points by concluding all worthy results:

- The maximum magnitude of stream function have been noticed with an enhanced in Da and porosity parameter for a fixed value of Ri, it is more augmented and marked for dominant free convective flows.
- The rise of thermal radiation parameter, higher value of stream function has been observed in the enclosure.
- The amplification in heat transfer has been noticed with an addition in Nr, Rd, ϕ and ϵ.
- For increasing the values of Hartmann number, Eckert number and Ri, the average Nusselt number also increases.
- The increase of Eckert number shows that temperature profile is expanding in the cavity and the θ_{avg} profile increases for greater values of Ha and Ri.

5.2 Future work

In future, this work may be extended in the following direction

- Impact of heat generation/absorbtion.
- Perform the non-stationary simulations.
- Apply the higher order finite elements in space.

Bibliography

[1] I. V. Koptyug, *MRI of mass transport in porous media:drying and sorption processes*, 2012, vol. 65.

[2] K. J. Dunn, D. J. Bergman, and G. A. LaTorraca, *Nuclear Magnetic Resonance:petrophysical and Logging Applications*, 2002, vol. 32.

[3] V. Costa, A. Sousa, and P. Vasseur, *Natural convection in square enclosures filled with fluid-saturated porous media under the influence of the magnetic field induced by two parallel vertical electric currents*, 2012, vol. 55.

[4] M. Rahman, H. F. Oztop, R. Saidur, A. Naim, and K. S. Al-Salem, *Heat and mass transfer in inclined semi-circular enclosures*, 2016, vol. 26.

[5] K. Okada and H. Ozoe, *Experimental heat transfer rates of natural convection of molten gallium suppressed under an external magnetic field in either the x, y, or z direction*, 1992, vol. 114.

[6] T. Grosan, C. Revnic, I. Pop, and D. B. Ingham, *Magnetic field and internal heat generation effects on the free convection in a rectangular cavity filled with a porous medium*, 2009, vol. 52.

[7] A. J. Chamkha, *MHD flow of a uniformly stretched vertical permeable surface in the presence of heat generation/absorption and a chemical reaction*, 2003, vol. 30.

[8] N. Rudraiah, R. Barron, M. Venkatachalappa, and C. Subbaraya, *Effect of a magnetic field on free convection in a rectangular enclosure*, 1995, vol. 33.

[9] J. Imberger and P. F. Hamblin, *Dynamics of lakes and reservoirs and cooling ponds*, 1982, vol. 14.

[10] M. A. Stanish, G. S. Schajer, and F. Kayihan, *A mathematical-model of drying for hygroscopic porous media*, 1986, vol. 32.

[11] A. G. Fedorov and R. Viskanta, *Three-dimensional conjugate heat transfer in the microchannel heat sink for electronic packaging*, 2000, vol. 43.

[12] C. K. Cha and Y. Jaluria, *Recirculating mixed convection flow for energy extraction*, 1984, vol. 27.

[13] L. A. B. Pilkington, *Review lecture: the float glass process.*

[14] K. Khanafer and A. Chamkha, *Mixed convection flow in a lid-driven enclosure filled with a fluid-saturated porous medium.* Elsevier, 1999, vol. 42, no. 13.

[15] T. Basak, P. V. K. Pradeep, S. Roy, and I. Pop, *Finite element based heat line approach to study mixed convection in a a porous square cavity with various wall thermal boundary conditions,*, 2011, vol. 54.

[16] V. Sivakumar, S. Sivasankaran, P. Prakash, and J. Lee, *Effect of heating location and size on mixed convection in lid-driven cavity*, 2010, vol. 59.

[17] S. Sivasankaran, V. Sivakumar, and P. Prakash, *Numerical study on mixed convection in a lid-driven cavity with non-uniform heating on both side walls*, 2010, vol. 53.

[18] A. C. Baytas, A. Liaqat, T. Gros, and I. Pop, *Conjugate natural convection in a square porous cavity*, 2001, vol. 37.

[19] N. H. Saeid, *Conjugate natural convection in a porous enclosure: effect of conduction in one of the vertical walls*, 2007, vol. 46.

[20] M. A. Sheremet and T. A. Trifonova, *Unsteady conjugate natural convection in a vertical cylinder containing a horizontal porous layer: Darcy model and Brinkman-extended Darcy model*, 2014, vol. 101.

[21] F. Garoosi, L. Jahanshaloo, M. M. Rashidi, A. Badakhsh, and M. E. Ali, *Numerical simulation of natural convection of the nanofluid in heat exchangers using a Buongiorno model*, 2015, vol. 254.

[22] D. Yadav, D. Nam, and J. Lee, *The onset of transient Soret-driven MHD convection confined within a Hele-Shaw cell with nanoparticles suspension*, 2016, vol. 58.

[23] B. H. Salman, H. A. Mohammed, K. M. Munisamy, and A. S. Kherbeet, *Characteristics of heat transfer and fluid flow in microtube and microchannel using conventional fluids and nanofluids: a review*, 2013, vol. 28.

[24] M. Sheikholeslami and D. D. Ganji, *Nanofluid convective heat transfer using semi analytical and numerical approaches: a review*, 2016, vol. 65.

[25] J. Koh and R. Colony, *Heat transfer of microstructure for integrated circuits*, 1986, vol. 13.

[26] M. Ghazvini and H. Shokouhmand, *Investigation of a nanofluid-cooled microchannel heat sink using fin and porous media approaches*, 2009, vol. 50.

[27] B. J. Gireesha, B. Mahanthesh, R. S. R. Gorla, and P. T. Manjunatha, *Thermal radiation and hall effects on boundary layer flow past a non-isothermal stretching surface embedded in porous medium with nonuniform heat source/sink and fluid-particle suspension*, 2015, vol. 52.

[28] A. Dogonchi, M. Alizadeh, and D. Ganji, *Investigation of MHD go-water nanofluid flow and heat transfer in a porous channel in the presence of thermal radiation effect*, 2017, vol. 28.

[29] T.Hayat, T. Muhammad, A.Alsaedi, and MS.Alhuthali, *Magnetohydrodynamic three-dimensional flow of viscoelastic nanofluid in the presence of nonlinear thermal radiation*, 2015, vol. 385.

[30] T.Hayat, S.Qayyum, M.Imtiaz, and A.Alsaedi, *Comparative study of silver and copper water nanofluids with mixed convection and nonlinear thermal radiation*, 2016, vol. 102.

[31] M. Sheikholeslami, *Magnetic field influence on nanofluid thermal radiation in a cavity with tilted elliptic inner cylinder*, 2017, vol. 229.

[32] K. Mehmood, S. Hussain, and M. Sagheer, *Mixed convection in alumina-water nanofluid filled lid-driven square cavity with an isothermally heated square blockage inside with magnetic field effect: Introduction.* Elsevier, 2017, vol. 109.

[33] M. Rahman, M. Alim, and M. Chowdhury, *Magnetohydrodynamic mixed convection around a heat conducting horizontal circular cylinder in a rectangular lid-driven cavity with Joule heating*, 2009, vol. 1, no. 3.

[34] M. Rahman, F. Hakan, N. Rahim, R. Saidur, and K. Al-Salem, *MHD mixed convection with Joule heating effect in a lid-driven cavity with a heated semi-circular source using the finite element technique*, 2011, vol. 60, no. 6.

[35] K. Mehmood, S. Hussain, and M. Sagheer, *Numerical simulation of MHD mixed convection in alumina–water nanofluid filled square porous cavity using KKL model: Effects of non-linear thermal radiation and inclined magnetic field.* Elsevier, 2017, vol. 238.

[36] Y. A. Cengel and J. M. Cimbala, *Fluid mechanics fundamentals and applications*, 2006, vol. 185201.

[37] D. F. Young, B. R. Munson, T. H. Okiishi, and W. W. Huebsch, *A brief introduction to fluid mechanics.* John Wiley & Sons, 2010.

[38] R. E. Sonntag, C. Borgnakke, G. J. V. Wylen, and S. V. Wyk, *Fundamentals of thermodynamics.* Wiley New York, 1998, vol. 6.

[39] R. K. Bansal, *A Text Book of Fluid Mechanics and Hydraulic Machines: In MKS and SI Units.* Laxmi Publications, 1998.

[40] J. P. Pritchard, C. J. Leylegian, and R. Fox, *Fox and McDonald's Introduction to Fluid Mechanics.* Hoboken: John Wiley & Sons, 2011.

[41] J. Kunes., *Dimensionless Physical Quantities in Science and Engineering.* Elsevier, 2012.

[42] W. M. Rohsenow, J. P. Hartnett, Y. I. Cho *et al.*, *Handbook of heat transfer*. McGraw-Hill New York, 1998, vol. 3.

[43] C. Johnson, *Numerical solution of partial differential equations by the finite element method*. Courier Corporation, 2012.

[44] C. Sivaraj and M. A. Sheremet, *Natural convection coupled with thermal radiation in a square porous cavity having a heated plate inside*, 2016, vol. 114.

[45] J. Koo and C. Kleinstreuer, *Viscous dissipation effects in microtubes and microchannels*, 2004, vol. 47.

[46] ——, *Laminar nanofluid flow in microheat-sinks*, 2005, vol. 48.

[47] S. Hussain, F. Schieweck, and S. Turek, *Efficient Newton multigrid solution techniques for higher order space time Galerkin discretizations of incompressible flow*, 2014, vol. 83.

[48] S. Hussain, K. Mehmood, and M. Sagheer, *MHD mixed convection and entropy generation of water-alumina nanofluid flow in a double lid driven cavity with discrete heating.*, 2016, vol. 419.

[49] S. Hussain, S. Ahmed, K. Mehmood, and M. Sagheer, *Effects of inclination angle on mixed convective nanofluid flow in a double lid-driven cavity with discrete heat sources*, 2017, vol. 106.

[50] M. A. Sheremet and I. Pop, *Mixed convection in a lid driven square cavity filled by a nanofluid: Buongiorno's mathematical model*, 2015, vol. 266.

[51] L. K. Saha, M. C. Somadder, and M. S. Uddin, *Mixed convection heat transfer in a lid driven cavity with wavy bottom surface*, 2014, vol. 1.

[52] G. F. Zheng, M. Y. Ha, H. S. Yoon, and Y. G. Park, *A numerical study on mixed convection in a lid-driven cavity with a circular cylinder*, 2013, vol. 27.

[53] E. Abu-Nada and A. J. Chamkha, *Mixed convection flow in a lid-driven inclined square enclosure filled with a nanofluid*, 2010, vol. 29.

[54] M. A. R. Sharif, *Laminar mixed convection in shallow inclined driven cavities with hot moving lid on top and cooled from bottom*, 2007, vol. 27.

[55] R. Iwatsu, J. M. Hyun, and K. Kuwahara, *Mixed convection in a driven cavity with a stable vertical temperature gradient*, 1993, vol. 36.